THERMAL SCALE MODELING OF THE TEMPERATURE CONTROL MODEL OF MARINER MARS 64

PHASE II TECHNICAL REPORT

JET PROPULSION LABORATORY
CONTRACT 950789
JANUARY 25, 1965

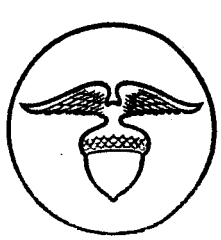

Arthur D. Little, Inc.

Sal 36099-R

THERMAL SCALE MODELING OF THE TEMPERATURE CONTROL MODEL OF MARINER MARS 64

Phase II Technical Report

to

Jet Propulsion Laboratory

Contract 950789

by

Frank Gabron
Robert W. Johnson
Arthur D. Little, Inc.

January 25, 1965

C-66326

Table of Contents

List of Tables

List of Figures

INTRODUCTION

The objective of the subject contract is to design, fabricate and test a one-half scale (approximately) thermal model of the Mariner Mars 64 Temperature Control Model (TCM). The tests of the Thermal Scale Model (TSM) will be made in a suitable simulated space environment at thermal equilibrium, and the measured temperatures compared with those measured by JPL for the full-scale TCM under conditions of thermal similitude. The contract requires that the temperatures measured for the TSM be submitted to JPL without prior knowledge of the temperatures obtained by JPL in similar tests with the full-scale TCM.

The total program is divided into three phases. Phase I, which was completed in July 1964, was a preliminary design effort. The problems associated with detailed design and fabrication of the TSM were studied, and a preliminary layout design for a 0.43 scale thermal model of the TCM was completed. This design was based on a set of thermal scaling laws which predict identical temperatures at homologous locations in model and prototype. Furthermore, the design of the model was based on the aim of the subject contract to produce a thermal scale model whose temperatures would correspond to those measured in the full-scale TCM tests within 5 degrees Fahrenheit.

During Phase II, a 0.43 scale model of the basic octagonal "bus" of the TCM was fabricated and tested in a thermal-vacuum chamber. The tests were made in a cold-wall (LN_2 temperature) vacuum chamber without solar simulation. The TSM tests were made at Arthur D. Little, Inc., in a five foot diameter chamber and corresponding tests of the TCM were

made by JPL in a 7 x 14 foot chamber. Temperature measurements at 48 locations (identical thermocouple locations were used in the TSM and TCM) were made at thermal equilibrium conditions.

This report contains a description of the Phase II TSM configuration and a description of ancillary tests that were made to establish the performance of a scaled thermal control louver assembly. In addition, a description of the theory and preliminary tests used to determine the procedures for thermally scaling the bolted joints is presented.

The Phase II test data--the temperatures measured in five tests of the TSM--are presented. Comparisons of the temperatures measured at homologous locations in the TSM and TCM are tabulated and discussed.

Phase III, which is the final phase of the subject contract, involves the design and fabrication of thermally scaled versions of the superstructure, solar panels and associated scientific experiments used on the TCM. The Phase III TSM configuration will be tested in early 1965 in the NASA Lewis Laboratory carbon-arc solar simulation facility, and the measured temperatures compared with those obtained by JPL with the TCM in the large JPL solar simulation facility. The Phase III configuration will thus essentially be a thermally scaled version of flight hardware.

SUMMARY

Experimental determinations of the equilibrium temperatures within a one-half scale thermal model of the Mariner Mars 64 spacecraft "bus" are reported.

The results of three separate tests of the model are compared with independent tests performed by Jet Propulsion Laboratory with a modified Mariner Mars 64 TCM under conditions of thermal similitude.

Two additional tests were performed with the model. The first test was performed to determine the influence of the heat leakage through small "gaps" between the thermal shields on the temperatures within the "bus". The second test was performed to determine the errors associated with temperature predictions made with a simplified version of a typical electronics bay.

Experimental results obtained in tests of the model and prototype showed that more than 50 percent of the temperatures corresponded within 5 deg. F., and 90 percent corresponded within 10 deg. F. Temperature differences across bolted joints were practically identical in model and prototype.

Eliminating the heat leakage through small "gaps" between the thermal shields resulted in a 5 degree Fahrenheit increase in the average temperature of the TSM. This result reveals the importance of the gap dimensions on the operating temperatures of both the TSM and TCM.

Substituting a simplified electronic chassis, in which all of the power was uniformly dissipated in a single heater, did not appreciably alter the temperatures within the spacecraft bus. This result suggests

possibilities for making further simplifications in fabricating thermal scale models.

It is concluded that temperatures within a complex spacecraft structure, typical of the Mariner vehicle, can be predicted by use of "temperature preservation" thermal scale modeling techniques to an accuracy useful for the verification of thermal design concepts.

The tests to be undertaken with a complete thermal scale model of the TCM in simulated sunlight should reveal the practicability of applying the technique to a complete spacecraft.

TECHNICAL DISCUSSION

A. Description of the Phase II Model

1. Introduction

In the Phase II test program, it was desired to obtain temperature comparisons between the TCM and TSM for the basic octagonal bus structure. Therefore, the TCM was modified by JPL for purposes of these special tests. The solar panels were removed, and the top and bottom surfaces of the bus were "superinsulated". The total internal power dissipated in the spacecraft would thus be emitted from the eight bays.

In previous solar simulation tests of the TCM (conducted by JPL) it was found that the uppermost thermal shield did not act as an adiabatic surface and the internal temperature of the bus was affected by the heat leaks through the thermal shield. Therefore, for the special tests conducted in the Phase II program, a heated "hat" section was installed on the top of the bus to increase the total internal power dissipation and thereby set the bus temperature within a normal operating temperature range.

The overall configuration of the Phase II TCM and TSM is shown in Figures 1 and 2. The model is practically identical to the TCM configuration with the exception of details which have been simplified and will be discussed in following sections of this report.

The TSM is geometrically similar to the TCM except that the dimensions are 43% of those of the TCM. The width across the flats of the octagonal frame is approximately 21 inches and the height of the bus is approximately 7 inches.

Five of the eight bays (Bays 1, 3, 4, 7, and 8) were equipped with temperature actuated thermal control louvers. These assemblies are variable emittance devices which increase the effective emittance of the bus with an increase in bus temperature. The louver assemblies used on the TSM were thermally scaled versions of those used on the TCM.

An overall view of Bay 2, which contains the Post Injection Propulsion System, is also shown in Figure 2.

Figure 3 shows the exterior of Bays 5, 6 and 7 (right to left) of the TSM. Bay 5 was completely shielded and Bay 6 was partially shielded. The exposed area of Bay 6 in the TSM was scaled from the exposed area of the TCM.

Top and bottom views, showing the interior of the TSM, are shown in Figures 4 and 5. These photographs were taken prior to final assembly and do not show the thermal control louvers or thermal shields. For comparison, a bottom view of the JPL TCM (attached to a mounting ring) is shown in Figure 6. It can be seen that much of the detail has been reproduced in the TSM with the exception of some additional wiring.

The similarity of the mounting of the power dissipating electronic sub-chassis in the TSM and TCM is shown in Figures 7 and 8. These interior views show some of the details in Bays 6, 7 and 8. The total internal power dissipated within the TSM was 27.21 watts.

In the following sections, we will discuss the procedures used in designing the TSM and the details of construction of the components.

2. Scaling Procedures

The TSM was designed in accordance with a set of thermal scaling laws which predict identical temperatures in model and prototype at homologous locations. The use of this "temperature preservation" technique was specified by Jet Propulsion Laboratory. In addition, it was desired to make model and prototype geometrically similar.

As it was desired to compare model and prototype temperatures at thermal equilibrium conditions, no consideration was given to the similitude parameters which govern transient scale modeling.

The theoretical basis for the design of thermal scale models of spacecraft has been established and the results of successful experiments with simplified thermal scale models--using the temperature preservation technique--have been presented in the literature [1].

The following relationships were used as a basis for the design of the TSM:

$$\frac{\epsilon_m}{\epsilon_p} = 1 \qquad (1)$$

$$\frac{\alpha_m}{\alpha_p} = 1 \qquad (2)$$

$$\frac{k_m}{k_p} = \frac{L_m}{L_p} = R \qquad (3)$$

$$\frac{C_m}{C_p} = 1 \qquad (4)$$

1. Fowle, A. A., et. al., Thermal Scale Modeling of Spacecraft: An Experimental Investigation, paper presented at AIAA Space Simulation Testing Conference, Pasadena, California, Nov. 16-18, 1964.

$$\frac{q_m}{q_p} = \left(\frac{L_m}{L_p}\right)^2 \qquad (5)$$

where

- ϵ - emittance
- α - absorptance
- k - thermal conductivity
- L - characteristic length
- R - geometric scale ratio
- C - thermal joint conductance
- q - rate of heat flow
- m - model
- p - prototype

Equations (1) and (2) require that identical emittances and absorptances be used in model and prototype. Equation (3) requires that the ratio of thermal conductivities be equal to the geometric scale ratio. Equations (4) and (5) require that the thermal conductances across bolted joints be identical and that the ratio of the rates of heat flow be proportional to the square of the geometric scale ratio.

In the design of the TSM, the emittances were made equal to those in the TCM by using the same surface finishes and paints. The materials of construction of the TSM were chosen to have thermal conductivities approximately 0.43 of those used in the TCM. The choice of a geometric scale ratio of 0.43, rather than, say, 0.5, was based on the availability of the particular materials which were used to fabricate the TSM. The joint conductances were made equal by design and test procedures to be discussed in a following section. Finally, the rates of heat flow in the

model were designed to be 0.1849 times the rates that existed in the prototype. In the Phase II configuration no external power was applied to the prototype and, therefore, Equation (5) was satisfied by simply scaling the internal power dissipation.

A further discussion of the details of the application of the scaling parameters to the components that comprise the TSM is given in the following sections.

3. Octagonal Bus Structure

The basic structural assembly consists of two octagonal frames bolted together with longerons. To this assembly are bolted the eight chassis plates (shear webs) which in turn support the electronic sub-chassis.

During the preliminary design phase of our work, several analyses were made to determine the relative effects of conduction and radiation in determining the temperature gradients within the entire structure. The results showed that the azimuthal temperature distribution in the bus is mainly determined by radiative effects, whereas conductive effects are important in determining the axial temperature distributions in the chassis plates and the temperature patterns in the regions where power dissipating sub-chassis are bolted to the chassis.

The shear webs were thus important with respect to conductive effects, and we chose to use SAE 1015 steel for fabricating the shear webs in the TSM.

The thermal conductivity of the ZK 60A magnesium TCM shear webs was estimated to be 1.21 watts/cm-K and SAE 1015 steel has a conductivity

of approximately 0.519 watts/cm-K. The geometric scale ratio was then set to be

$$\frac{L_m}{L_p} = \frac{k_m}{k_p} = \frac{0.519}{1.21} = 0.43$$

This geometric scale factor was then applied to all of the dimensions of the TCM to arrive at the proper dimensions of the TCM.

The octagonal frames were machined from an Alloy 9B aluminum bronze casting. This composition is reported [1] to have a conductivity of 0.63 watts/cm-K which is 52% of the conductivity of the magnesium used in the TCM. A drawing of the top frame section is shown in Figure 9. The webs that were cast in this frame structure were not required from the thermal standpoint but were provided for the attachment of equipment to be used in the Phase III program.

The details of the shear webs are shown in Figure 10. These plates were geometrically scaled in thickness from those used in the TCM and were fabricated from SAE 1015 steel. As shown in Figure 10, several of the shear webs were designed with varying thicknesses. Because of the importance of conductance effects in determining the temperature distributions within the shear webs, a scaled geometry was used in the TSM, although some changes in the radii of the machined patterns were made for ease of fabrication.

The magnesium longerons in the TCM were also thermally scaled by using 1015 steel and scaled wall thicknesses in the TSM. Instead of

1. Metals Handbook, Volume 1, Properties and Selection of Metals, 1961.

fabricating the longerons from a single casting, the TSM longerons were made from weldments as shown in Figure 11.

4. Packaging Assembly

There are seven bays that dissipate power in the TCM--Bay II houses the PIPS and does not have any internal power. Of those that dissipate power, Bays VI, VIII and I dissipate 39, 20 and 14 percent of the total internal power, respectively. Because of the wide variation in internal power between bays, we simplified the electronic packaging in those bays or modules that have small power dissipations. Since each bay was treated in a slightly different manner, we will discuss the layout of each bay in turn in the following paragraphs.

The individual modules are radiatively coupled to one another and are conductively coupled to the shear web through bolted joints. The emittance of the TSM modules is approximately the same as the corresponding TCM modules. Gold plated boxes were used where required and the emittance of the Dow 7 used on the TCM was reproduced by a black oxide finish.

The modules that dissipate more than 1 watt (in the TCM) have scaled radiating areas and conduction paths. For these TSM modules, the number of shear web bolted connections were identical to the number used in the TCM. The only geometrical difference between these TSM modules and those used in the TCM was the location of the horizontal divider to which the heater was attached. In the TSM the divider was located at the bottom of the module instead of on a central plane. These modules were made from SAE 1015 steel with scaled wall thicknesses.

The modules in the TCM which dissipate less than one watt or have no power dissipation were not exactly scaled in the TSM. The maximum temperature rise of these modules if they are conductively decoupled will be only 3 to 4 degrees C per watt of power dissipation. Therefore, certain liberties were taken in modeling these modules. In these cases, the modules were bolted to the shear web face but did not have the bolted tab connections. These modules were fabricated from SAE 1015 steel and had scaled wall thicknesses. These modules were similar in shape to the higher power modules except that two of the vertical sides were omitted. This change did not appreciably affect the radiative coupling between bays or modules, and did represent a considerable simplification with respect to manufacturing.

Heaters and thermistors were affixed to each module in the same relative locations as on the TCM. Each module was equipped with a disconnect to facilitate the removal of a complete chassis assembly.

We will now discuss the characteristics of each chassis in turn.

A packaging assembly drawing for Bay I is shown in Figure 12. This bay contains scaled versions of modules that dissipate more than and less than one watt in the TCM. In Figure 12 the scaled powers for each component are identified with the JPL identification as noted on the JPL drawing J 4901042. The powers were obtained from the appropriate scaling ratio of $(0.43)^2$ which is 0.185. (A listing of the TSM powers and the thermocouple list used is presented in Appendix I.) An example of the module construction we used for those TCM modules that dissipate more than one watt is module 4A13. Examples of the simulation of

modules that dissipate less than one watt in the TCM are modules 8A1/8A2. One of these is shown in section A-A of Figure 12.

In Figures 13 and 14 are shown the layouts of Bays III and IV. The layout of Bay III is similar to the TCM with the exceptions previously noted. In order to simulate the gap between boxes 3A1 and 6A8 on the TCM, we combined the powers of modules 3A1 and 3A5, and modules 6A8 and 6A10. This change is noted in Figure 14.

The assembly of Bay V is shown in Figure 15. The bay contains two low emittance boxes, viz., 2RA2 and 2RA1 which dissipate rather large amounts of power. Module 16A1--which does not dissipate power--was simulated by use of a single plate bolted to the vertical members of the shear web. In the TCM this module was not bolted to the shear web face and we are merely representing the radiation blockage between the interior of the shear web face and the interior of the bus.

The assembly of Bay VI is shown in Figure 16. This bay has a larger amount of power than any other bay, and also contains component 2PA1 which singly dissipates more power than any other module or component.

The assembly layout of Bay VII is shown in Figure 17. In the TCM, the attitude control electronics are attached to the left side of Bay VII. We have simulated this component by a single module having the same approximate shape. This representation is shown in Figure 17 as module 7A1. The remaining modules were reasonable thermal versions of those used in the TCM except that the area occuped by the gyro control (7A2) in the TCM was simulated by two smaller modules.

The layout of Bay VIII is shown in Figure 18. In this bay the heaters were directly attached to the dividers and the shear web face as in the TCM. The locations of the heaters are noted. In this particular drawing we have not shown the cover that blocks the Bay VIII shear web from viewing the interior of the bus.

5. Scaling of Bolted Joints

In our studies [1] of the problems associated with the thermal design of scaled bolted joints, it was shown that the bolt load in the model should be equal to the bolt load in the prototype multiplied by the scaling ratio--which in this case is 0.43. This conclusion is based on the assumption that the mating surfaces are thermally scaled, and that the hardness and surface roughness are nearly identical in model and prototype. However, our studies also showed that the temperature differences between the sub-chassis and the chassis plates were in large part controlled by the "constriction resistance" in the chassis plate. This constriction resistance is due to the fact that the heat flow patterns in the chassis are governed by the conductance of the chassis. In this case the temperature differences across the bolted joints are more strongly influenced by the area of contact and the thermal conductance of the chassis than by the actual temperature difference across the metal-to-metal interface.

The basic approach used to scale the bolted joint thermal performance involved the use of reduced size bolts, torqued to a scaled

---

1. Thermal Scale Modeling of the Mariner Mars 64 Spacecraft, Phase IB Preliminary Report to Jet Propulsion Laboratory, July 2, 1964.

load. For example, the #8-32 titanium bolts (35 inch-lb torque) used to join the chassis to frame were modeled by use of #6-32 stainless bolts torqued to approximately 7 inch-pounds. The #6-32 stainless bolts (18 inch-lb torque) used to attach the power dissipating sub-chassis to the chassis plates were modeled by use of #4-40 stainless steel bolts torqued to 5.5 inch-pounds. The bolt sizes and torques used in the TSM were selected to have a scaled bolt load of approximately 43% of the load that existed in the corresponding bolts of the TCM. The loads were estimated from the friction torque characteristics of bolts presented in the literature [1].

In recognizing the uncertainties involved in basing the joint designs on limited theory and approximate calculations of friction coefficients, etc., we completed a series of ancillary tests to determine whether the basic approach stated above would be applicable to the thermal scaling of the joints between the power dissipating modules (sub-chassis) and the chassis.

A TCM sub-chassis was bolted (in accordance with JPL specifications) to a 10 inch diameter magnesium plate of approximately the same thickness as the TCM chassis. A 25 watt heater was installed in the sub-chassis, and the sub-chassis and back of the 10 inch plate were "super-insulated". The assembly was placed in a small vacuum chamber with a liquid nitrogen cooled interior shroud and temperature differences across the bolted joint were measured. The 10 inch plate was used to radiate the 25 watts to the cooled vacuum chamber shroud. A 0.43 scale

1. Belford, R. B., et. al., Joint Design, Machine Design, March 21, 1963.

TSM sub-chassis and a scaled radiating plate (both were fabricated from 1015 steel) were assembled in accordance with the scaling methods discussed previously. The power input to the TSM chassis was scaled to be 4.6 watts. This assembly was also used to make temperature difference measurements in the vacuum chamber.

The full scale assembly was used to investigate the effects of bolt torque, bolt material and the conductance of the radiating plate on the temperature differences from the sub-chassis to the radiating plate.

The basis of comparison for the tests was the temperature difference measured with the TCM sub-chassis attached to the magnesium plate with three #6-32 stainless steel bolts torqued to 18 inch-pounds. The measured temperature difference for this configuration was 83.5 F with 25 watts of internal power dissipation. (The mean fourth power temperature of the radiating plate was used to arrive at the temperature differences.) Reducing the bolt torque to 9 inch-pounds increased the temperature difference to 107.3 F. Changing the bolt material from stainless to titanium (at the same torque) did not affect the temperature difference. Increasing the thermal conductance of the radiating plate by substituting a copper plate of the same thickness as the magnesium plate--thereby increasing the conductance by a factor of about three--decreased the temperature difference from 83.5 F to 41 F. This result shows the importance of scaling the conductive paths around the bolted regions.

From the results of these tests with the full-scale bolted joint assembly, we concluded that the scaling of the conductive paths (i.e., the constriction resistance) and the bolt torque would be important in determining the temperature patterns in the scaled sub-chassis.

Next, the TSM sub-chassis assembly was tested to determine whether or not the temperature differences would correspond with those measured in the full-scale assembly. It was desired to have the temperature differences in the TSM assembly correspond with those measured in the TCM assembly with the magnesium radiating plate and the bolts torqued to 18 inch-pounds as this configuration is typical of the fully assembled TCM.

The scaled TSM sub-chassis was bolted to the scaled radiating plate with three #4-40 stainless screws torqued to 5.5 inch-pounds. The measured temperature difference was 69.8 F which was lower than the 83.5 F difference measured with the TCM sub-chassis. Reducing the torque to 2.7 inch-pounds increased the difference to 88.9 F. At this point, we could have chosen to set the bolt torques at about 4.7 inch-pounds and this presumably would have set the temperature difference to correspond with the TCM sub-chassis assembly at 83.5 F. However, we decided to investigate one additional variable, viz., the size of the clearance hole in the radiating plate since we had rather arbitrarily used a clearance hole diameter of 0.125 inches in this test setup. The clearance hole was enlarged to 0.149 inches and the temperature difference increased from 69.8 F to 93.4 F (at 5.5 inch-pounds of torque). This surprising result showed that the geometry of

the hole pattern was influential in determining the temperature distribution for these sub-chassis. If the temperature difference is assumed to be linear with clearance hole diameter, a 0.136 inch clearance hole diameter in the TSM assembly (with a bolt torque of 5.5 inch-pounds) would make the temperature differences in model and prototype correspond.

The holes for the sub-chassis bolts in the TSM chassis plates were drilled to this diameter and the bolt torques set at 5.5 inch-pounds.

We anticipated that the thermally scaled joint problem would be most critical for the bolted modules that dissipated relatively large amounts of power in the TCM. Therefore, we did not complete any experiments with the joints between the frame and chassis plates. In this case, we believed that only small amounts of power would be transferred between the frame and chassis and that the temperature differences would be small.

In conclusion, we thermally scaled the bolted joints by use of a limited amount of theory and the results of ancillary tests with a full-scale JPL sub-chassis and a 0.43 thermal scale model of the sub-chassis. The results of these tests were used to determine bolt torques and clearance hole diameters which would provide temperature difference correspondence in model and prototype.

6. Thermal Control Louvers

The five sets of thermal control louvers used on the TCM are used to regulate the bus temperatures. The normal operating temperature range is from 55 to 80 F. The louver blades are fabricated from polished aluminum which has a low infrared emittance. In the closed position the blades shield the spacecraft bus. As the blades open, the chassis--which is painted to have a high emittance--is exposed, thereby increasing the effective emittance of the assembly. At temperatures below 55 F, the louver blades are closed and the assembly has an effective emittance of 0.12. At temperatures above 80 F, the louver blades are wide open and the effective emittance of each assembly is 0.76. At 55 F a typical set of louvers will radiate 6.9 watts of power and at 80 F the power dissipation will be 52.6 watts. These results were obtained from JPL tests [1].

Each pair of louver blades on a TCM assembly is driven by a bi-metallic spring which will rotate approximately 90 degrees with a temperature change of 25 F. The bi-metallic actuating springs are radiatively coupled to the chassis of the spacecraft so that the angular position of the blades is a function of the chassis temperature. Each set of blades can be adjusted within a small range to set the temperature at which the blades open.

In the tests completed by JPL with the modified TCM, the louver blades on the assemblies mounted on Bays 7 and 8 were set to open at 55 F and on Bays 1, 3 and 4, the blades were set to open at 63 F.

1. Mariner Louver Performance, Interoffice Memo by M. Gram, January 15, 1964.

In designing the louver assemblies for the TSM, it was decided to utilize the same method for controlling the blade angles and to retain, as closely as possible, the geometrical characteristics of the TCM assemblies. The design of the TSM louvers was thus based on a requirement to have eleven pairs of individually actuated blades in each assembly. The scaling laws (c.f. page 7) require that the emittances be identical in model and prototype, and that the ratio of conductivities be equal to the scaling ratio. However, in the case of the louvers, the power dissipated is controlled by radiative rather than conductive effects. Therefore, the TSM louvers were made from the same material, polished aluminum, to have essentially the same emittance as the prototype TCM assembly.

An exploded view of a typical blade assembly for the 0.43 scale TSM louvers is shown in Figure 19. This figure shows the bi-metallic actuating spring, the micarta axle and nylon bushings used to support the assembly. A view of a partially assembled set of blades is shown in Figure 20. A fully assembled set of louvers, complete with center section housing, is shown in Figure 3.

In designing the TSM louver assemblies at 0.43 scale, two problems were encountered. First, bi-metallic springs less than half the size of those used in the TCM were not readily available. Therefore, the dimensions of the center section housing the springs were larger than a scaled dimension thus reducing the effective radiating area of the exposed chassis with the blades in the open position. Second, in small bi-metal spring sizes, the maximum available rotation was

3 degrees of rotation per degree F temperature change. The TCM springs produced 3.6 degrees of rotation per degree F of temperature change. Therefore, the temperature span associated with the fully closed to fully open blade position was 5 F greater in the TSM.

To examine the thermal performance of a typical "scaled" TSM louver assembly, an extra assembly was fabricated for testing. The power dissipation vs. temperature characteristics of a TCM louver assembly were known from JPL tests and it was desired to compare these results--on a scaled basis--with the measured performance of a TSM louver assembly.

The power dissipation vs. temperature characteristics of a TSM louver assembly were measured in a vacuum bell jar with a liquid nitrogen cooled "black" inner shroud. The louver assembly was mounted on an aluminum plate to which was affixed a heating element. The aluminum plate was painted with PV 100[1] paint (also used on the TCM) on the side facing the louver assembly and insulated with multi-foil super-insulation on the other side. By measuring the temperature of the aluminum plate and measuring the input power to the heater, the thermal performance of the louver was obtained over a wide range of temperatures. For this particular setup, the opening temperature of the louver blades was set at approximately 55 F. A comparison of the TCM louver and TSM louver performance is shown in Figure 21. The upper curve is based on JPL data scaled by Equation 5 (page 7) which requires that the power be scaled in proportion to the geometric scale ratio

1. Vita-Var Paint Co., Orange, N. J., #15966.

(0.43) squared. The experimental data obtained with the scaled TSM louver indicate that the effective radiating area was low. Between the fully closed and open blade positions, the differences can be attributed in part to spring characteristics and the problems associated with "sticking" blades. The effective radiating area of the TSM louvers was known to be approximately 10% low because of the additional non-scaled area of the center housing. Therefore, to increase the effective radiating area of the assemblies used on the TSM, the chassis were painted with 3-M Optical Black Velvet paint instead of PV 100 paint. The emittance of PV 100 was measured to approximately 0.85. The emittance of 3-M paint was approximately 0.95. The substitution of this paint thus increased the effective radiating area by 10%. No additional experiments were made on the louver assembly with the 3-M painted surface since this correction was relatively straightforward. The temperature correspondence between model and prototype at a given power level was estimated to be of the order of 5 F which was of the same order as the experimental error. On the basis of this limited test program, it was decided to use the TSM configuration without further refinements to produce exact temperature correspondence. The reasons for making this decision were twofold. Tests of each of the five TCM and TSM louvers would be required to make precise comparisons, and the use of five assemblies on the spacecraft tends to "smear out" differences in the temperatures of individual bays.

It should be noted that in the assembly of the five sets of louvers used on the TSM, the angular position of the blades was

adjusted by setting the blades in the fully open position corresponding to the "fully open" temperature of the TCM assemblies. This approach was taken since the internal temperature of the spacecraft is more sensitive to changes in effective emittance when the louvers are at or near the fully open position.

7. Post Injection Propulsion System

The PIPS consists of a group of propellant and pressurant tanks, a rocket engine and associated controls. The entire bay containing the PIPS system--as installed on the TCM--is thermally isolated from the external environment by low emittance surfaces except for the "black cavity" produced by the rocket exhaust nozzle. Since no power is dissipated within the bay and the power radiated from the bay is small due to the low effective emittance of the exterior surfaces, errors associated with thermally modeling the system will have little influence on the temperatures of the other seven bays. For this reason, the TSM design was based on an approach which would simulate the gross thermal behavior and, therefore, many simplifications were made in designing a thermal mockup of the PIPS.

A drawing illustrating the TSM PIPS configuration is shown in Figure 22. The geometry of the system was retained, however, much of the detail used on the TCM such as piping, rocket motor insulation, etc., was omitted from the TCM. The conductive paths in the exhaust nozzle and jet vane support were approximately scaled from the thermal standpoint, however, it was recognized that the temperatures within the system would tend to "float". That is, because of the use of low

conductivity materials and low emittances, the temperatures within the nozzle, for example, are extremely sensitive to small changes in heat flux. In the following discussion of the comparison of temperatures measured for the TCM and TSM, it will be shown that the temperature correspondence between model and prototype in this particular bay was poorer than in any other location.

8. Insulation and Paint Treatments

The top and bottom of the spacecraft bus were insulated by use of multi-foil superinsulation. Approximately 12 layers of aluminized Mylar separated by silk netting were used as an insulation package. A similar system of insulation--from the thermal standpoint--was used on the TCM. In this particular spacecraft configuration, small heat leaks associated with the superinsulation package have little influence on the internal temperatures because of the large amounts of power radiated from the large areas of high emittance on the sides.

The thermal shields mounted on the sides of the TCM were made of polished aluminum and were thermally "shorted" to the bus by aluminum standoffs with bolts. Polished aluminum shields of approximately the same thickness were used on the TSM. They were also thermally short-circuited to the bus. Again, because of the large amounts of power dissipated by the unshielded bays, the influence of differences in the thermal coupling and emittances of the shields is small from the standpoint of predicting interior temperatures.

Three types of paint were used on the interior of the TCM and the same paint treatments were applied to the interior portions of the TSM.

The interior surfaces of the bus and the longerons were painted with Cat-A-Lac[1] Flat Black 463-3-8. The exterior portions of the longerons were painted with Cat-A-Lac Gloss White 443-1-500. The exterior surfaces of the chassis were painted with PV 100 White[2]. To insure that the emittances in model and prototype were equivalent, the emittances of several samples of each surface--painted by JPL to flight specifications--were compared with samples of the same paint prepared by ADL. The relative emittances were determined by calorimetric techniques using the ADL Emissometer. The results showed that the maximum difference in the relative emittance was 1.2% for the three paints which have total hemispherical emittances at room temperature ranging from 0.847 to 0.886.

1. Finch Paint Co., Torrance, California.
2. Vita-Var Paint Co., Orange, New Jersey.

B. Phase II Test Procedures

1. Description of Tests

The Phase II test program consisted of the experimental determination of the TSM "bus" temperatures for three different test conditions. These TSM tests were performed in a thermal-vacuum chamber at Arthur D. Little, Inc. Solar simulation was not used in these tests. Three corresponding tests were performed by Jet Propulsion Laboratory using a modified TCM. The temperatures at 48 locations within the "bus" were measured at thermal equilibrium. The location of the temperature measurements was identical in TCM and TSM.

Jet Propulsion Laboratory provided information on the TCM internal power, the power supplied to the TCM "hat section" for each test, and the measured temperatures of the TCM "hat section". The measured TCM bus temperatures were supplied to ADL following the submission of the measured TSM temperatures to Jet Propulsion Laboratory.

The three tests undertaken in Phase II were designed to provide information on the accuracy of the thermal scale model in three different situations. In each of the three tests, the amount of power dissipated in the "bus" was maintained constant at the "Earth Cruise" condition.

In Test 1, the power supplied to the "hat section" was made relatively small with respect to the power dissipated in the "bus" in order to set the average bus temperature within the normal operating temperatures of the thermal control louver assemblies. The purpose of this test was to compare the measured temperature distributions of the TCM and TSM when the louver assemblies were partially open.

In Test 2, the power supplied to the hat section was increased to set the average "bus" temperature at or above the "fully open" position of the thermal control louver assemblies. The purpose of this test was to compare the measured temperature distributions at elevated temperature levels when the thermal control function of the louver assemblies was removed.

In Test 3, two of the thermal control louver assemblies were caged in the fully-open position (Bays 1 and 3) and the remaining three assemblies were caged in the fully-closed position (Bays 4, 7, 8). The purpose of this test was to compare temperature distributions in the TCM and TSM when the bus temperature gradients were intentionally made large by forcing most of the internal power to be emitted by the two bays with caged open louver assemblies.

In addition to the three aforementioned tests, two additional tests were performed with the TSM. The first of these supplementary tests, Test 3A, was performed to evaluate the influence of "heat leaks" associated with gaps between the "flight-type" thermal shields on the temperatures of the TSM. During the installation of the thermal shields on the TSM, it was recognized that differences in the relative gap dimensions between the TSM and TCM could exist because of tolerance limits in the manufacture and final assembly of the shields. The gaps between the thermal shields, which act as "black-body" cavities, were covered with a low emittance aluminized tape and Test 3 was repeated in order to assess the influence of these "heat leak" paths on the TSM temperatures.

The second additional test of the TSM, Test 4, was performed to determine the influence of substituting a simplified version of Bay 6 for the complicated assemblage of simulated electronic sub-chassis. Test 4 was performed under the same conditions as Test 3, viz., with two louver assemblies caged fully open and the remaining assemblies caged closed. A view of the interior assembly of Bay 6, as used in Test 3, is shown in Figure 23. The modified Bay 6 configuration used in Test 4 is shown in Figure 24. This single heater dissipated the same amount of power as the total amount dissipated in the five sub-chassis used in the Test 3 configuration.

The internal powers that were dissipated in each test of the modified TCM and the TSM and the positions of the thermal control louver assemblies are presented in Table I.

2. Test Equipment and Measurements

The TSM tests were conducted in a five foot diameter thermal-vacuum chamber with an interior shroud cooled to liquid nitrogen temperatures. The interior surface of the shroud was coated with an optical black paint to produce a high infrared emittance. During the TSM tests the internal pressure in the chamber was maintained in the 10^{-6} torr range.

Power was supplied to the TSM by use of a 300 volt DC power supply with 0.007 percent regulation. The individual heaters used within the TSM were precision wire-wound power resistors. Power measurements were made by current and resistance measurements. It was estimated that the total power measurements were accurate to within 0.09 percent.

The temperatures were measured by use of calibrated, matched thermistors. The entire lot of thermistors had resistance vs. temperature characteristics such that any single thermistor would have an error of less than $\pm$ 1/2 F over the temperature range of 32 to 212 F when a single resistance vs. temperature curve was used. Calibrations were made by the vendor to establish the resistance vs. temperature curve and three point calibrations of each thermistor were made by Arthur D. Little, Inc., as acceptance tests. These calibrations showed that the maximum error was less than $\pm$ 1/2 F.

A constant current of 30 microamps was supplied to the thermistors. The voltages were read on a digital voltmeter. The voltages were translated to temperature by use of a digital computer data reduction program. It was estimated that the total system error in measuring the temperatures was of the order of $\pm$ 1/2 F.

Temperature measurements of the TSM were recorded at approximately one hour time intervals. The final steady-state temperature measurements were made when the change in any temperature between three successive readings was less than 0.1 F. The time required for the TSM to reach thermal equilibrium varied with the test condition, however, the average time was approximately 12 hours.

C. Test Results

The measured temperatures for the three tests of the modified TCM and the TSM are presented in Tables II, III, and IV. In each table, the temperature differences between the TSM and the TCM measured at homologous locations are tabulated.*

Comparisons of the average temperatures in each bay for the three tests are presented in Table V. Comparisons of the temperature levels of each bay in the TCM and TSM were made by computing the average of all of the temperature measurements within a given bay. The percentage errors in the average temperatures of the TSM bays were based on the average absolute temperatures of the TCM bays.

In Table VI, data are presented for the temperature differences between four electronic sub-chassis and the shear webs to which they are mounted. Comparisons of the measured temperature differences for each of the three TCM and TSM tests are presented.

Comparisons of measured chassis temperatures in Test 1 of the TSM and TCM are made in Table VII.

Tables VIII and IX contain data on the two tests made only with the TSM. A comparison of Tests 3 and 3A--which were used to determine the influence of heat leakage paths in the thermal shields--is made in Table VIII.

The effect of making a simplified version of the Bay 6 heater arrangement is shown in Table IX. In this table, the TSM temperatures measured in Tests 3 and 4 are compared.

* Thermocouple #324 was not recorded in the JPL tests of the TCM. The temperatures at the same location measured in the TSM are listed for reference.

D. Discussion of Test Results

This discussion of the test results must be prefaced by the remark that the prediction of the spacecraft bus temperatures by use of the one-half scale thermal model was remarkably good. Generally speaking, the results show that the temperatures within a spacecraft structure, typical of the Mariner Mars 64, could be predicted by thermal modeling techniques to within 5 degrees Fahrenheit.

In reviewing the data obtained in all of the tests, there were only three temperature measurements that fell outside of the limits of accuracy generally required for thermal design purposes. These three temperature measurements were made within the Post Injection Propulsion System and the umbilical connector. A simplified thermal model of the PIPS was used in the TSM, and the umbilical connector was "mocked-up" rather than scaled from the thermal standpoint.

The approach used in designing and fabricating the Thermal Scale Model was based on the objective of accurately predicting the temperatures of bus structure and the electronic sub-chassis, particularly those having a high internal power dissipation. For this reason, considerable emphasis was placed on the scaling of the thermal control louver assemblies and the bolted joints through which large amounts of power are being transferred.

The data indicate that this objective was met with considerable success.

The detailed temperature comparisons for the Phase II test program will be discussed in the following paragraphs.

The results of Test 1--a test in which all louvers were free to operate normally--indicate that the average absolute error in the TSM temperatures was 5.2 F, or one percent of the absolute temperature. (The absolute values of all differences were summed and averaged over the 44 bus temperature measurements.) Four temperatures were in error by 10 F or greater and only ten were in error by more than 6 F. In particular, the largest errors were encountered in Bay 2. The maximum error was 31.5 F as measured in the rocket nozzle. The errors associated with Bay 2 measurements are due to the relatively poor thermal coupling between these elements and the remainder of the spacecraft, and the fact that no internal power is dissipated in Bay 2. Furthermore, because of the large temperature gradients in these areas the temperature correspondence between TCM and TSM is subject to larger errors.

In Test 1, the temperature correspondence in the Bays with high internal power, such as Bays 6 and 8, is extremely good although in general the model ran slightly lower in temperature than the TCM. In a following discussion of Tests 3 and 3A, it will be shown that the presence of non-scaled gaps between the thermal shields--which act as "black-body" cavities--caused the model temperatures to be slightly low.

The results of Test 2 show that the temperature errors follow the same pattern as in Test 1; however, as expected the errors are slightly larger because of the higher temperature level and the fact that the thermal control function of the louver assemblies was deleted by driving the louvers wide open at these high temperature levels. The average absolute error between the TCM and TSM for Test 2 was 7.7 F, or

about 1.4 percent of the absolute temperature level. The "hat" temperature measurements showed that the "hat section" in the model was nearly 30 degrees F colder than the TCM. The power to the "hat section" was appropriately scaled and small heat leaks in the super-insulation on the top of the hat would not result in a difference of this magnitude. An examination of the details of the TSM and TCM indicated that the TCM had proportionately more radiative blockage between the hat and the bus. The blockage is due to the presence of wiring, connections, and the cable troughs. This effect would tend to decrease the hat temperatures of the TSM for a properly scaled power dissipation in the hat itself.

Test 3 forms the basis of a temperature comparison with increased temperature gradients in the bus and with the louvers on three bays caged closed. The average absolute error between the TCM and TSM was 4.7 F in Test 3. This is slightly less than the error in Test 1. The test results showed that the temperature differences across the octagonal bus were significantly altered. The temperature difference between Bays 3 and 7--on opposing sides of the octagonal structure--was less than 5 F in Test 1 and over 40 F in Test 3. A conclusion that can be drawn from the comparisons of Tests 1 and 3 is that the accuracy of the temperature predictions is preserved when the temperature differences between bays are increased by an order of magnitude. This result is appropriate to considerations of the application of thermal modeling techniques to other spacecraft designs where temperature gradients within the structure are significant.

The comparison of average bay temperatures as presented in Table V summarizes the errors in average temperature correspondence. The average bay temperatures correspond to within one percent for Tests 1 and 3 and the maximum error is less than 1.5 percent.

The comparison of the temperature differences across four electronic sub-chassis, as presented in Table VI, indicates that the modeling of the joint conductances was within the experimental accuracy of the measurements.* The temperature drop across the bolted joint in sub-chassis 2PA1--which has a large power dissipation--corresponded to within two degrees. Similar correspondence was obtained for sub-chassis 2PS1 which had a joint temperature drop of nearly 30 degrees F.

The temperatures of the chassis, i.e., the shear webs, are compared in Table VII for Test 1. The average absolute error of the 16 measurements was 3.3 degrees F. The results indicate that the accuracy of temperature predictions was of the same order as the accuracy of the experimental measurements.

The influence of the heat leakage paths between the gaps in the thermal shields is shown in the data presented in Table VIII for Tests 3 and 3A. These test results were obtained in two similar tests of the TSM. The data indicate that covering the gaps in the thermal shields with low emittance aluminized tape increased the average temperature level of the model by about 5 degrees F. However, in Bay 3 the temperature level was increased by about 10 degrees F. It was noted that the measured temperatures in Bay 3 of the TSM were disproportionately lower

* The accuracy of the TCM measurements was estimated to be $\pm$ 1 F by JPL. The accuracy of the TSM measurements was estimated to be $\pm$ 1/2 F.

than the other bays when compared to the TCM results. The results of Test 3A indicate that part of the error was due to "non-scaled" gaps between the thermal shields used on Bay 3. It should be noted that dimensional tolerances associated with these gaps are significant from the thermal standpoint. Deviations in the "gap areas" of two full-scale spacecraft or a model of the full-scale spacecraft can result in appreciable temperature differences.

The results of Test 4, which was made with a simplified version of Bay 6, point out the fact that a complicated bay can be simplified without appreciable error in the temperatures. The chassis temperatures in Bay 6 were within a few degrees of the Test 3 results with either the TSM or TCM. This change did not appreciably alter the temperatures of the remainder of the bus. Therefore, in future thermal modeling studies, one should consider the possibilities of using simplified heating arrangements to determine structural temperatures.

TABLE I

SUMMARY OF TEST CONDITIONS

	Test 1	Test 2	Test 3	Test 3A	Test 4
Power (watts)					
TCM Bus	147.37	147.37	147.37	-	-
TCM Hat	23.6	264.0	50.2	-	-
TCM TOTAL	170.97	411.37	197.57		
TSM Bus	27.21	27.21	27.21	27.21	27.21
TSM Hat	4.36	48.81	9.28	9.28	9.28
TSM TOTAL	31.57	76.02	36.49	36.49	36.49
Louver Positions					
Bay 1	Free	Free	Caged Open	Caged Open	Caged Open
Bay 3	Free	Free	Caged Open	Caged Open	Caged Open
Bay 4	Free	Free	Caged Closed	Caged Closed	Caged Closed
Bay 7	Free	Free	Caged Closed	Caged Closed	Caged Closed
Bay 8	Free	Free	Caged Closed	Caged Closed	Caged Closed

TABLE II

COMPARISON OF TEMPERATURE RESULTS--TEST 1

JPL TC NO.	BAY NO.	LOCATION	TSM (ADL) T_m (°F)	TCM (JPL) T_p (°F)	$T_m - T_p$
242	-	Bus Tube, Bottom	72.8	78.0	- 5.2
243	-	Bus Tube, Top	73.0	78.0	- 5.0
245	4	N_2 Bottle, Top	73.2	79.0	- 5.8
246	8	N_2 Bottle, Bottom	73.1	77.0	- 3.9
248	1	4A15	83.6	84.0	- 0.4
249	1	Chassis, 4A15	73.5	77.0	- 3.5
250	1	4A13	83.6	81.0	2.6
303	1	4A17	67.7	68.0	- 0.3
305	2	Nozzle Throat	49.5	18.0	31.5
306	2	Jet Vane Ring	40.0	57.0	-17.0
307	2	Prop. Tank	65.5	71.0	- 5.5
309	2	Umbilical	15.4	3.0	12.4
310	2	Shear Plate	58.1	59.0	- 0.9
311	3	33A2	70.7	80.0	- 9.3
316	3	32A4	70.2	81.0	-10.8
322	3	Chassis C/L Top	65.2	71.0	- 5.8
323	3	Chassis C/L Center	63.8	70.0	- 6.2
324	3	Chassis C/L Bottom	61.9	-	-
329	4	6A13	82.2	77.0	5.2
330	4	Chassis, 6A13	75.1	74.0	1.1
332	4	6A9	68.1	63.0	5.1
333	4	Flight	70.8	76.0	- 5.2
336	5	2TR1	80.3	86.0	- 5.7
337	5	2RA1	83.7	86.0	2.3
340	5	Chassis C/L Top	76.6	81.5	- 4.9
341	5	Chassis C/L Center	77.9	82.0	- 4.1
342	5	Chassis C/L Bottom	77.0	81.5	- 4.5
345	6	2PA1 Case	101.0	110.5	- 9.5
347	6	Chassis, 2PA1	84.4	93.0	- 8.6
348	6	2PS1	108.0	108.5	- 0.5
349	6	Chassis, 2PS1	82.1	80.0	2.1
350	6	2RE1	91.2	87.5	3.7
401	6	Chassis C/L Top	83.0	84.0	- 1.0
402	6	Chassis C/L Center	79.8	79.0	0.8
403	6	Chassis C/L Bottom	83.4	87.5	- 4.1
406	7	7A1	77.7	72.5	5.2
412	7	7A2	66.2	66.5	- 0.3
415	7	5A8	73.5	72.0	1.5
418	7	Flight	67.1	66.5	0.6
419	8	Diodes, Upper	73.1	66.5	6.6
420	8	Diodes, Lower	70.1	64.5	5.6
422	8	Booster, Upper	93.8	91.5	2.3
423	8	C/L Top	69.2	67.5	1.7
425	8	C/L Bottom	67.6	64.5	3.1
426	8	Battery Cover	72.1	71.5	0.6
451	-	Hat, Center	76.2	83.0	- 6.8

TABLE III

COMPARISON OF TEMPERATURE RESULTS--TEST 2

JPL TC NO.	BAY NO.	LOCATION	TSM (ADL) T_m (°F)	TCM (JPL) T_p (°F)	$T_m - T_p$
242	-	Bus Tube, Bottom	145.1	160.0	- 14.9
243	-	Bus Tube, Top	139.1	151.0	- 11.9
245	4	N_2 Bottle, Top	147.8	159.0	- 11.2
246	8	N_2 Bottle, Bottom	126.7	143.0	- 16.3
248	1	4A15	104.2	111.0	- 6.8
249	1	Chassis, 4A15	96.1	102.5	- 6.4
250	1	4A13	103.4	117.0	- 13.6
303	1	4A17	91.5	97.5	- 6.0
305	2	Nozzle Throat	95.3	64.0	31.3
306	2	Jet Vane Ring	83.8	109.5	- 25.7
307	2	Prop. Tank	120.0	134.0	- 14.0
309	2	Umbilical	45.8	32.0	13.8
310	2	Shear Plate	108.2	100.0	8.2
311	3	33A2	107.6	118.0	- 10.4
316	3	32A4	96.1	111.0	- 14.9
322	3	Chassis C/L Top	95.8	101.0	- 5.2
323	3	Chassis C/L Center	85.3	90.0	- 4.7
324	3	Chassis C/L Bottom	85.0	-	-
329	4	6A13	119.7	109.0	10.7
330	4	Chassis, 6A13	110.8	102.5	8.3
332	4	6A9	95.5	84.0	11.5
333	4	Flight	99.2	103.0	- 3.8
336	5	2TR1	138.9	144.0	- 5.1
337	5	2RA1	134.3	138.0	- 3.7
340	5	Chassis C/L Top	133.8	136.0	- 2.2
341	5	Chassis C/L Center	130.1	134.0	- 3.9
342	5	Chassis C/L Bottom	126.3	131.0	- 4.7
345	6	2PA1 Case	144.7	157.0	- 12.3
347	6	Chassis, 2PA1	129.9	141.0	- 11.1
348	6	2PS1	152.6	155.0	- 2.4
349	6	Chassis, 2PS1	126.3	124.0	2.3
350	6	2RE1	133.1	132.0	1.1
401	6	Chassis C/L Top	134.3	135.5	- 1.2
402	6	Chassis C/L Center	123.7	123.5	0.2
403	6	Chassis C/L Bottom	127.9	134.0	- 6.1
406	7	7A1	114.0	112.0	2.0
412	7	7A2	95.0	102.0	- 7.0
415	7	5A8	112.2	112.0	0.2
418	7	Flight	95.4	99.0	- 3.6
419	8	Diodes, Upper	103.7	96.0	7.7
420	8	Diodes, Lower	95.0	93.0	2.0
422	8	Booster, Upper	122.2	118.0	4.2
423	8	C/L Top	99.4	95.0	4.4
425	8	C/L Bottom	89.9	90.5	- 0.6
426	8	Battery Cover	114.0	115.0	- 1.0
451	-	Hat, Center	185.2	214.0	- 28.8

TABLE IV

COMPARISON OF TEMPERATURE RESULTS--TEST 3

JPL TC NO.	BAY NO.	LOCATION	TSM (ADL) T_m (°F)	TCM (JPL) T_p (°F)	$T_m - T_p$
242	-	Bus Tube, Bottom	74.5	80.0	- 5.5
243	-	Bus Tube, Top	73.9	78.5	- 4.6
245	4	N_2 Bottle, Top	74.8	79.5	- 4.7
246	8	N_2 Bottle, Bottom	73.6	77.5	- 3.9
248	1	4A15	63.5	64.5	- 1.0
249	1	Chassis, 4A15	51.9	54.5	- 2.6
250	1	4A13	63.6	62.5	1.1
303	1	4A17	46.4	46.5	- 0.1
305	2	Nozzle Throat	38.1	9.0	29.1
306	2	Jet Vane Ring	29.8	45.5	- 15.7
307	2	Prop. Tank	55.3	60.5	- 5.2
309	2	Umbilical	-0.1	-10.5	10.4
310	2	Shear Plate	45.6	39.5	6.1
311	3	33A2	48.1	55.5	- 7.4
316	3	32A4	45.5	57.5	- 12.0
322	3	Chassis C/L Top	40.9	44.0	- 3.1
323	3	Chassis C/L Center	35.0	37.5	- 2.5
324	3	Chassis C/L Bottom	35.1	-	-
329	4	6A13	82.0	73.5	8.5
330	4	Chassis, 6A13	74.0	69.5	4.5
332	4	6A9	65.2	69.5	- 4.3
333	4	Flight	68.8	71.5	- 2.7
336	5	2TR1	82.9	87.5	- 4.6
337	5	2RA1	85.6	87.5	- 1.9
340	5	Chassis C/L Top	78.6	82.0	- 3.4
341	5	Chassis C/L Center	79.5	82.0	- 2.5
342	5	Chassis C/L Bottom	78.2	81.5	- 3.3
345	6	2PA1 Case	103.8	113.5	- 9.7
347	6	Chassis, 2PA1	87.5	95.5	- 8.0
348	6	2PS1	111.9	112.5	- 0.6
349	6	Chassis, 2PS1	86.9	85.0	1.9
350	6	2RE1	95.7	93.0	2.7
401	6	Chassis C/L Top	87.6	89.0	- 1.4
402	6	Chassis C/L Center	83.8	83.5	0.3
403	6	Chassis C/L Bottom	87.7	91.5	- 3.8
406	7	7A1	88.1	83.5	4.6
412	7	7A2	77.2	79.0	- 1.8
415	7	5A8	86.2	85.5	0.7
418	7	Flight	80.8	81.5	- 0.7
419	8	Diodes, Upper	85.9	80.5	5.4
420	8	Diodes, Lower	82.0	77.5	4.5
422	8	Booster, Upper	98.6	95.5	3.1
423	8	C/L Top	81.2	80.0	1.2
425	8	C/L Bottom	78.1	75.0	3.1
426	8	Battery Cover	77.9	75.5	2.4
451	-	Hat, Center	83.8	94.0	- 10.2

TABLE V

COMPARISON OF AVERAGE BAY TEMPERATURES

BAY I

LOUVERED

Internal Power (Earth Cruise)	TCM 20.898 watts		TSM 3.864 watts
	Test 1	Test 2	Test 3
TCM (JPL)	77.5F	107.0F	57.0F
TSM (ADL)	77.0F	98.8F	56.4F
Error in Model Temperature (%)	-0.093	-1.446	-0.116

BAY II

POST INJECTION PROPULSION SYSTEM

Internal Power	TCM 0.0 watts		TSM 0.0 watts
	Test 1	Test 2	Test 3
TCM (JPL)	41.6F	87.9F	28.8F
TSM (ADL)	45.7F	90.6F	33.9F
Error in Model Temperature (%)	+0.817	+0.493	+1.044

BAY III

LOUVERED

Internal Power (Earth Cruise)	TCM 9.118 watts		TSM 1.686 watts
	Test 1	Test 2	Test 3
TCM (JPL)	70.8F	96.6F	45.0F
TSM (ADL)	66.4F	93.9F	40.9F
Error in Model Temperature (%)	-0.829	-0.485	-0.811

TABLE V (Continued)

BAY IV

LOUVERED

Internal Power (Earth Cruise) TCM 15.036 watts TSM 2.779 watts

	Test 1	Test 2	Test 3
TCM (JPL)	72.5F	99.6F	71.0F
TSM (ADL)	74.1F	106.3F	72.5F
Error in Model Temperature (%)	+0.300	+1.197	+0.282

BAY V

SHIELDED

Internal Power (Earth Cruise) TCM 6.500 watts TSM 1.202 watts

	Test 1	Test 2	Test 3
TCM (JPL)	83.4F	136.6F	84.1F
TSM (ADL)	79.1F	132.7F	80.9F
Error in Model Temperature (%)	-0.791	-0.654	-0.588

BAY VI

PARTIALLY SHIELDED

Internal Power (Earth Cruise) TCM 56.607 watts TSM 10.466 watts

	Test 1	Test 2	Test 3
TCM (JPL)	91.3F	137.8F	95.4F
TSM (ADL)	89.1F	134.1F	93.1F
Error in Model Temperature (%)	-0.399	-0.619	-0.414

TABLE V (Continued)

BAY VII

LOUVERED

Internal Power (Earth Cruise)	TCM 9.615 watts		TSM 1.775 watts
	Test 1	Test 2	Test 3
TCM (JPL)	69.4F	106.3F	82.4F
TSM (ADL)	71.1F	104.2F	83.1F
Error in Model Temperature (%)	+0.321	-0.370	+0.110

BAY VIII

LOUVERED

Internal Power (Earth Cruise)	TCM 29.600 watts		TSM 5.473 watts
	Test 1	Test 2	Test 3
TCM (JPL)	71.0F	101.3F	80.7F
TSM (ADL)	74.3F	104.0F	83.9F
Error in Model Temperature (%)	+0.621	+0.481	+0.592

TABLE VI

COMPARISON OF TEMPERATURE DIFFERENCES ACROSS BOLTED JOINTS

Electronic Sub-chassis 4A15

Internal Power	TCM 8.26 watts		TSM 1.527 watts
	Test 1	Test 2	Test 3
Differential Temperature TCM (JPL)	7.0F	8.5F	10.0F
Differential Temperature TSM (ADL)	10.1F	8.1F	11.6F

Electronic Sub-chassis 6A13

Internal Power	TCM 6.70 watts		TSM 1.239 watts
	Test 1	Test 2	Test 3
Differential Temperature TCM (JPL)	3.0F	6.5F	4.0F
Differential Temperature TSM (ADL)	7.1F	8.9F	8.0F

Electronic Sub-chassis 2PA1

Internal Power	TCM 26.8 watts		TSM 4.955 watts
	Test 1	Test 2	Test 3
Differential Temperature TCM (JPL)	17.5F	16F	18F
Differential Temperature TSM (ADL)	16.6F	14.8F	16.3F

Electronic Sub-chassis 2PS1

Internal Power	TCM 20.1 watts		TSM 3.716 watts
	Test 1	Test 2	Test 3
Differential Temperature TCM (JPL)	28.5F	31F	27.5F
Differential Temperature TSM (ADL)	25.9F	26.3F	25.0F

TABLE VII

COMPARISON OF CHASSIS TEMPERATURE RESULTS--TEST 1

JPL TC NO.	BAY NO.	LOCATION	TSM (ADL) T_m (°F)	TCM (JPL) T_p (°F)	$T_m - T_p$
249	1	Chassis 4A15	73.5	77.0	- 3.5
310	2	Shear Plate	58.1	59.0	- 0.9
322	3	Chassis C/L Top	65.2	71.0	- 5.8
323	3	Chassis C/L Center	63.8	70.0	- 6.2
324	3	Chassis C/L Bottom	61.9	-	-
330	4	Chassis 6A13	75.1	74.0	+ 1.1
340	5	Chassis C/L Top	76.6	81.5	- 4.9
341	5	Chassis C/L Center	77.9	82.0	- 4.1
342	5	Chassis C/L Bottom	77.0	81.5	- 4.5
347	6	Chassis 2PA1	84.4	93.0	- 8.6
349	6	Chassis 2PS1	82.1	80.0	+ 2.1
401	6	Chassis C/L Top	83.0	84.0	- 1.0
402	6	Chassis C/L Center	79.8	79.0	+ 0.8
403	6	Chassis C/L Bottom	83.4	87.5	- 4.1
418	7	Flight (Chassis)	67.1	66.5	+ 0.6
423	8	C/L Top	69.2	67.5	+ 1.7
425	8	C/L Bottom	67.6	64.5	+ 3.1

TABLE VIII

COMPARISON OF TSM TEMPERATURES--TESTS 3 AND 3A

(Gaps in thermal shields taped in Test 3A.)

JPL TC NO.	BAY NO.	LOCATION	TSM TEMPERATURES (°F) Test 3A	Test 3	Difference
242	-	Bus Tube, Bottom	81.2	74.5	6.7
243	-	Bus Tube, Top	80.5	73.9	6.6
245	4	N_2 Bottle, Top	81.6	74.8	6.8
246	8	N_2 Bottle, Bottom	80.1	73.6	6.5
248	1	4A15	69.6	63.5	6.1
249	1	Chassis, 4A15	58.1	51.9	6.2
250	1	4A13	69.9	63.6	6.3
303	1	4A17	53.1	46.4	6.7
305	2	Nozzle Throat	45.3	38.1	7.2
306	2	Jet Vane Ring	36.6	29.8	6.8
307	2	Prop. Tank	63.2	55.3	7.9
309	2	Umbilical	10.7	- 0.1	10.8
310	2	Shear Plate	53.0	45.6	7.4
311	3	33A2	58.0	48.1	9.9
316	3	32A4	57.2	45.5	11.7
322	3	Chassis C/L Top	51.7	40.9	10.8
323	3	Chassis C/L Center	46.6	35.0	11.6
324	3	Chassis C/L Bottom	45.3	35.1	10.2
329	4	6A13	89.8	82.0	7.8
330	4	Chassis, 6A13	82.0	74.0	8.0
332	4	6A9	73.6	65.2	8.4
333	4	Flight	76.9	68.8	8.1
336	5	2TR1	89.2	82.9	6.3
337	5	2RA1	92.1	85.6	6.5
340	5	Chassis C/L Top	85.3	78.6	6.7
341	5	Chassis C/L Center	86.3	79.5	6.8
342	5	Chassis C/L Bottom	85.1	78.2	6.9
345	6	2PA1 Case	108.7	103.8	4.9
347	6	Chassis, 2PA1	92.8	87.5	5.3
348	6	2PS1	116.8	111.9	4.9
349	6	Chassis, 2PS1	91.9	86.9	5.0
350	6	2RE1	101.0	95.7	5.3
401	6	Chassis C/L Top	92.9	87.6	5.3
402	6	Chassis C/L Center	88.8	83.8	5.0
403	6	Chassis C/L Bottom	93.1	87.7	5.4
406	7	7A1	94.6	88.1	6.5
412	7	7A2	83.8	77.2	6.6
415	7	5A8	92.7	86.2	6.5
418	7	Flight	87.3	80.8	6.5
419	8	Diodes, Upper	92.0	85.9	6.1
420	8	Diodes, Lower	88.1	82.0	6.1
422	8	Booster, Upper	104.1	98.6	5.5
423	8	C/L Top	86.9	81.2	5.7
425	8	C/L Bottom	83.9	78.1	5.8
426	8	Battery Cover	84.1	77.9	6.2

TABLE IX

COMPARISON OF TSM TEMPERATURES--TESTS 3 AND 4
(Modified Bay 6 heater in Test 4.)

JPL TC NO.	BAY NO.	LOCATION	TSM TEMPERATURES (°F) Test 3	Test 4	Difference
242	-	Bus Tube, Bottom	74.5	72.9	1.6
243	-	Bus Tube, Top	73.9	72.3	1.6
245	4	N_2 Bottle, Top	74.8	73.2	1.6
246	8	N_2 Bottle, Bottom	73.6	72.0	1.6
248	1	4A15	63.5	61.9	1.6
249	1	Chassis, 4A15	51.9	50.3	1.6
250	1	4A13	63.6	61.9	1.7
303	1	4A17	46.4	44.6	1.8
305	2	Nozzle Throat	38.1	36.1	2.0
306	2	Jet Vane Ring	29.8	28.1	1.7
307	2	Prop. Tank	55.3	53.7	1.6
309	2	Umbilical	- 0.1	3.3	-3.4
310	2	Shear Plate	45.6	42.4	3.2
311	3	33A2	48.1	45.4	2.7
316	3	32A4	45.5	43.7	1.8
322	3	Chassis C/L Top	40.9	39.0	1.9
323	3	Chassis C/L Center	35.0	33.5	1.5
324	3	Chassis C/L Bottom	35.1	33.6	1.5
329	4	6A13	82.0	80.8	1.2
330	4	Chassis, 6A13	74.0	72.7	1.3
332	4	6A9	65.2	63.6	1.6
333	4	Flight	68.8	67.2	1.6
336	5	2TR1	82.9	82.9	0.0
337	5	2RA1	85.6	84.7	0.9
340	5	Chassis C/L Top	78.6	78.2	0.4
341	5	Chassis C/L Center	79.5	78.8	0.7
342	5	Chassis C/L Bottom	78.2	77.3	0.9
345	6	2PA1 Case	103.8	-	-
347	6	Chassis, 2PA1	87.5	-	-
348	6	2PS1	111.9	-	-
349	6	Chassis, 2PS1	86.9	87.7	-0.8
350	6	2RE1	95.7	-	-
401	6	Chassis C/L Top	87.6	91.1	-3.5
402	6	Chassis C/L Center	83.8	86.0	-2.2
403	6	Chassis C/L Bottom	87.7	87.5	0.2
406	7	7A1	88.1	86.9	1.2
412	7	7A2	77.2	75.4	1.8
415	7	5A8	86.2	84.2	2.0
418	7	Flight	80.8	79.1	1.7
419	8	Diodes, Upper	85.9	83.7	2.2
420	8	Diodes, Lower	82.0	79.9	2.1
422	8	Booster, Upper	98.6	96.7	1.9
423	8	C/L Top	81.2	78.8	2.4
425	8	C/L Bottom	78.1	75.9	2.2
426	8	Battery Cover	77.9	76.0	1.9
451	-	Hat, Center	83.8	82.1	1.7

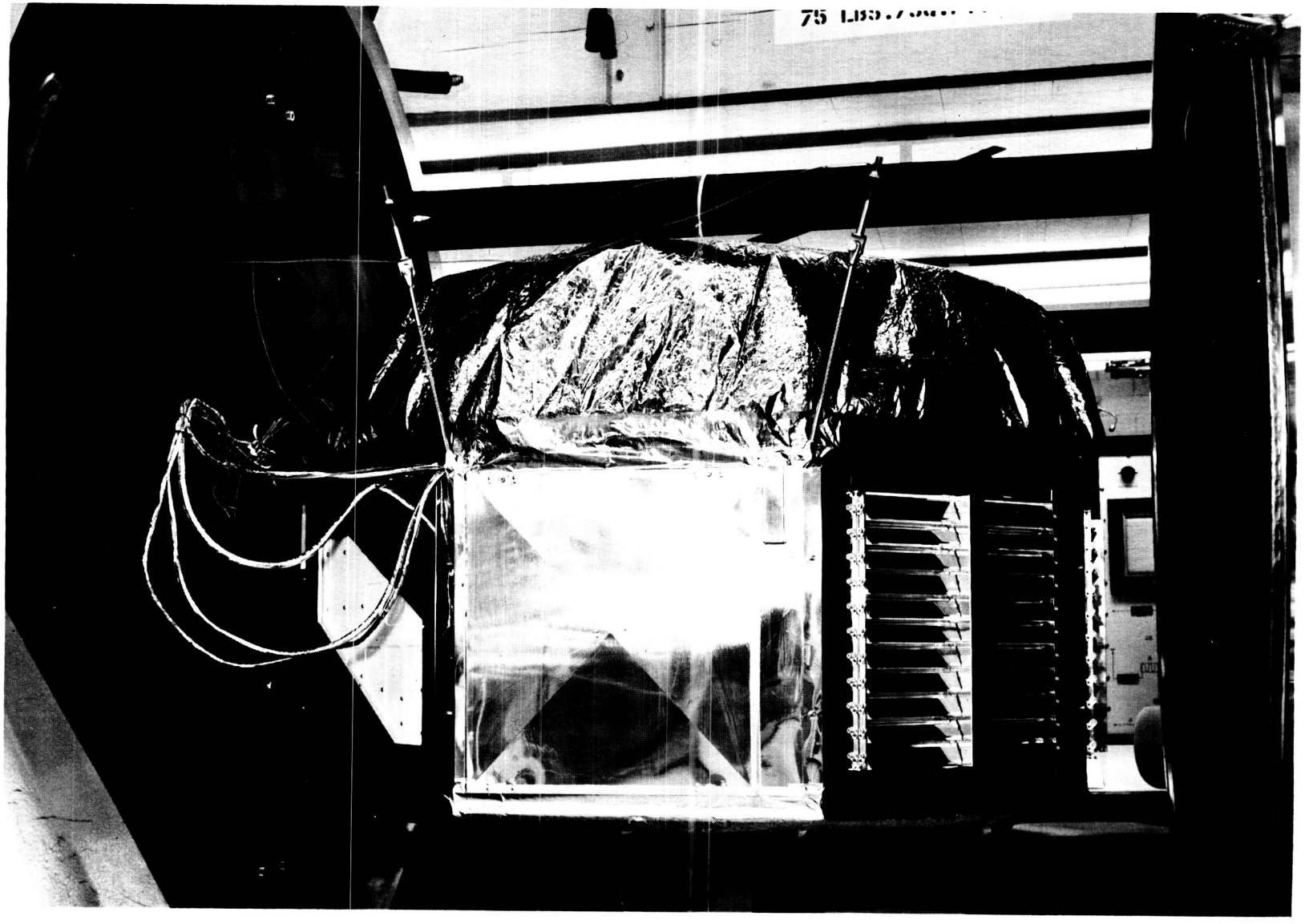

FIGURE 1 TEMPERATURE CONTROL MODEL - PHASE II CONFIGURATION

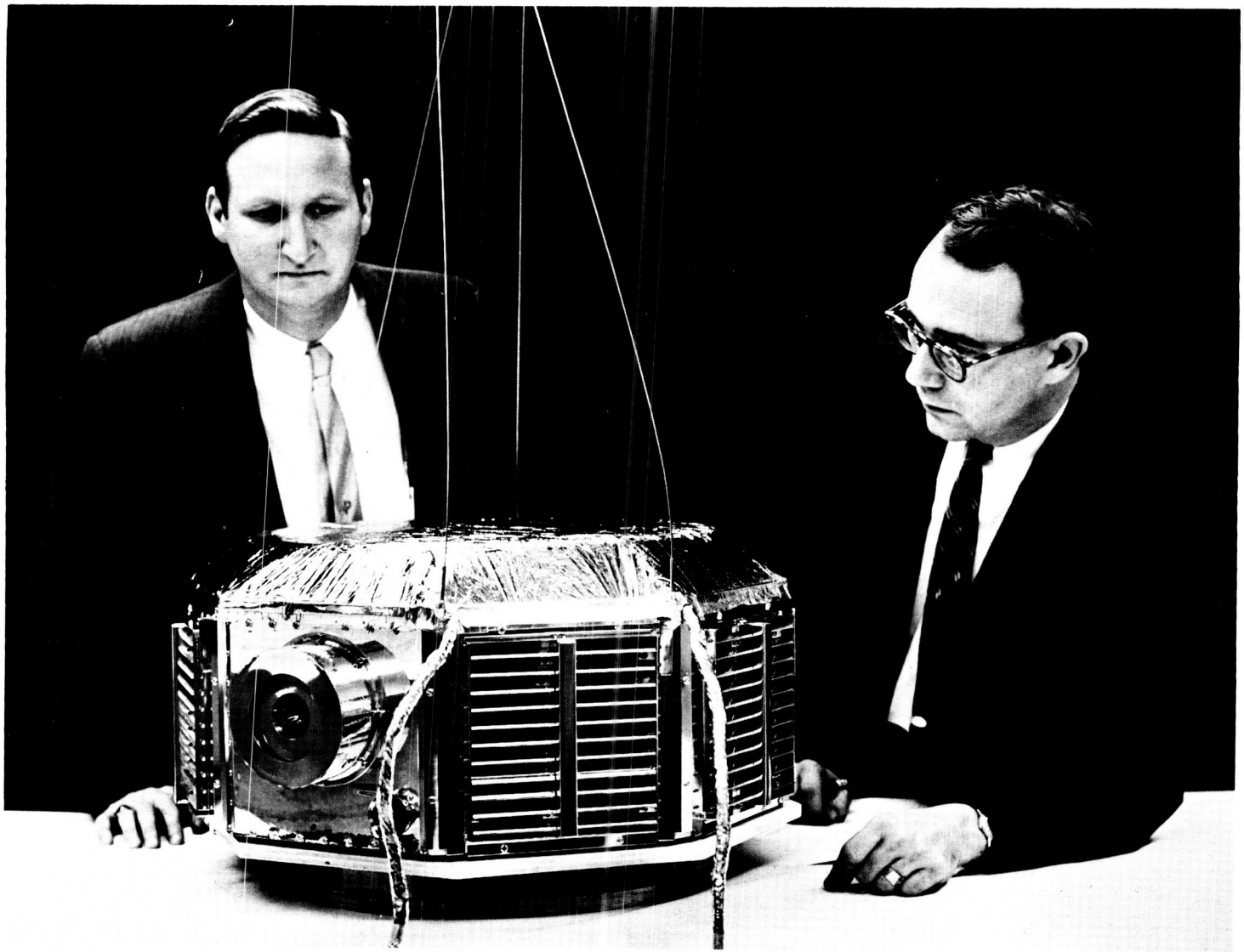

FIGURE 2 THERMAL SCALE MODEL

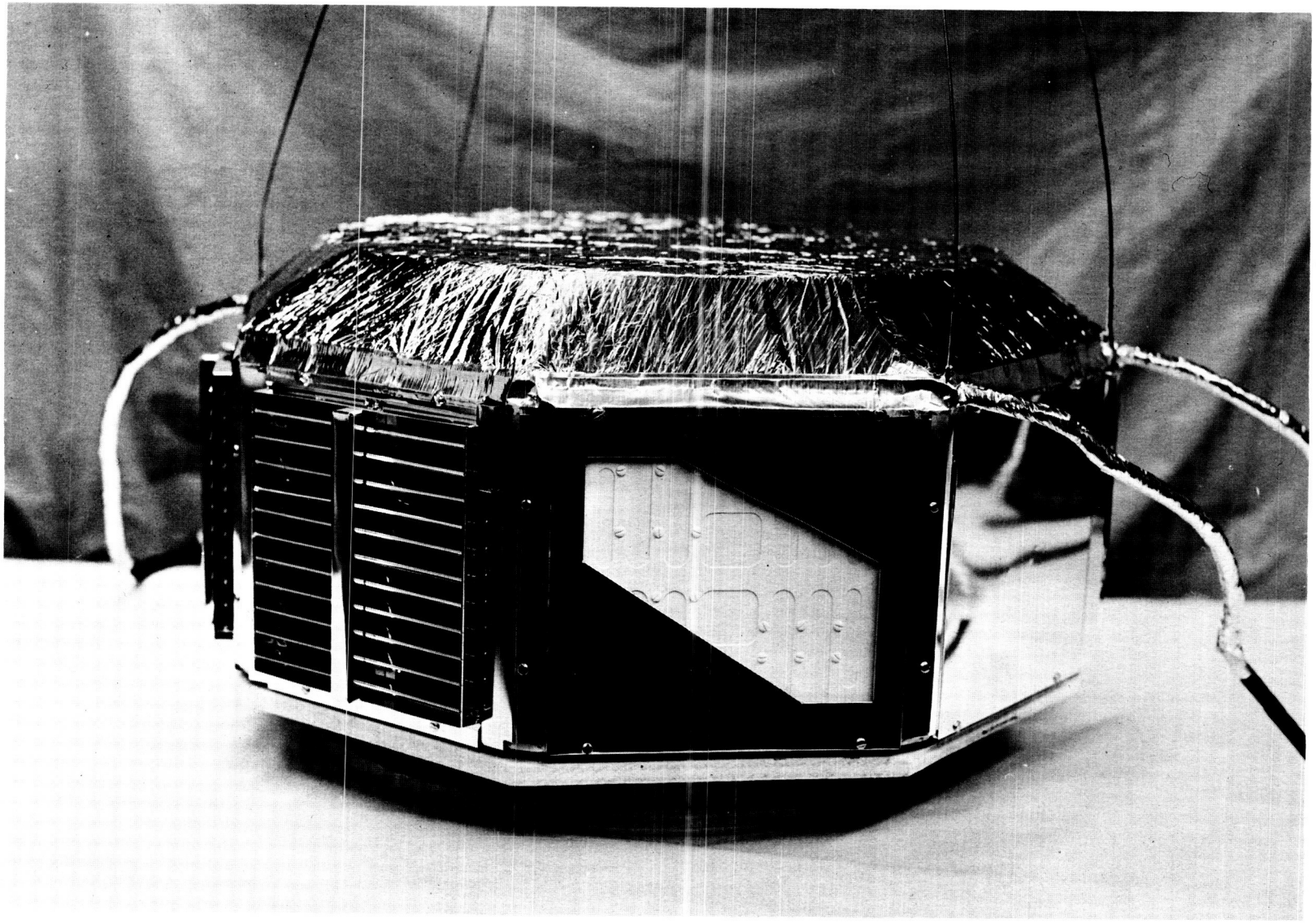

FIGURE 3 THERMAL SCALE MODEL (BAYS 5, 6, 7)

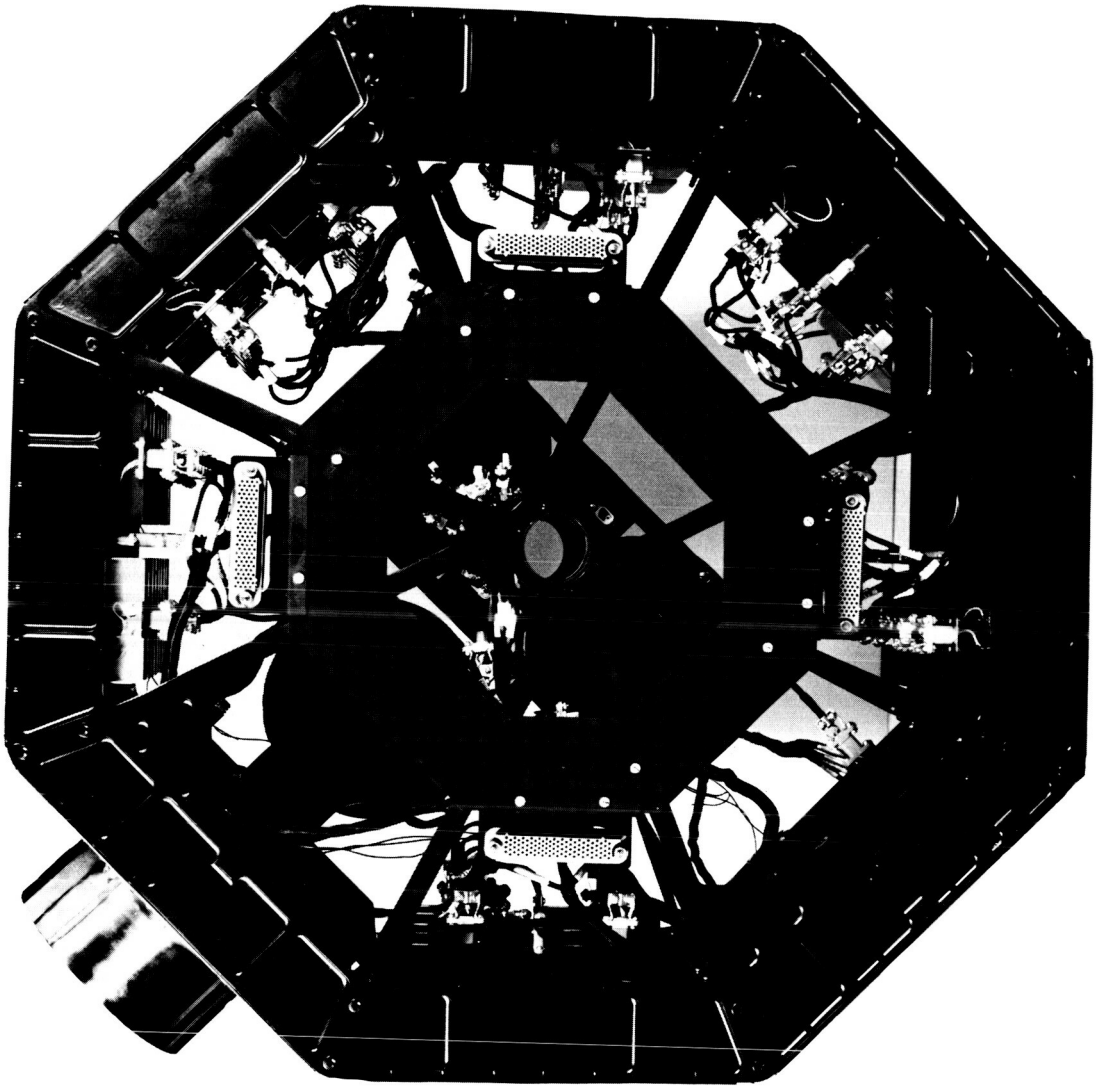

FIGURE 4 TOP VIEW - TSM BUS

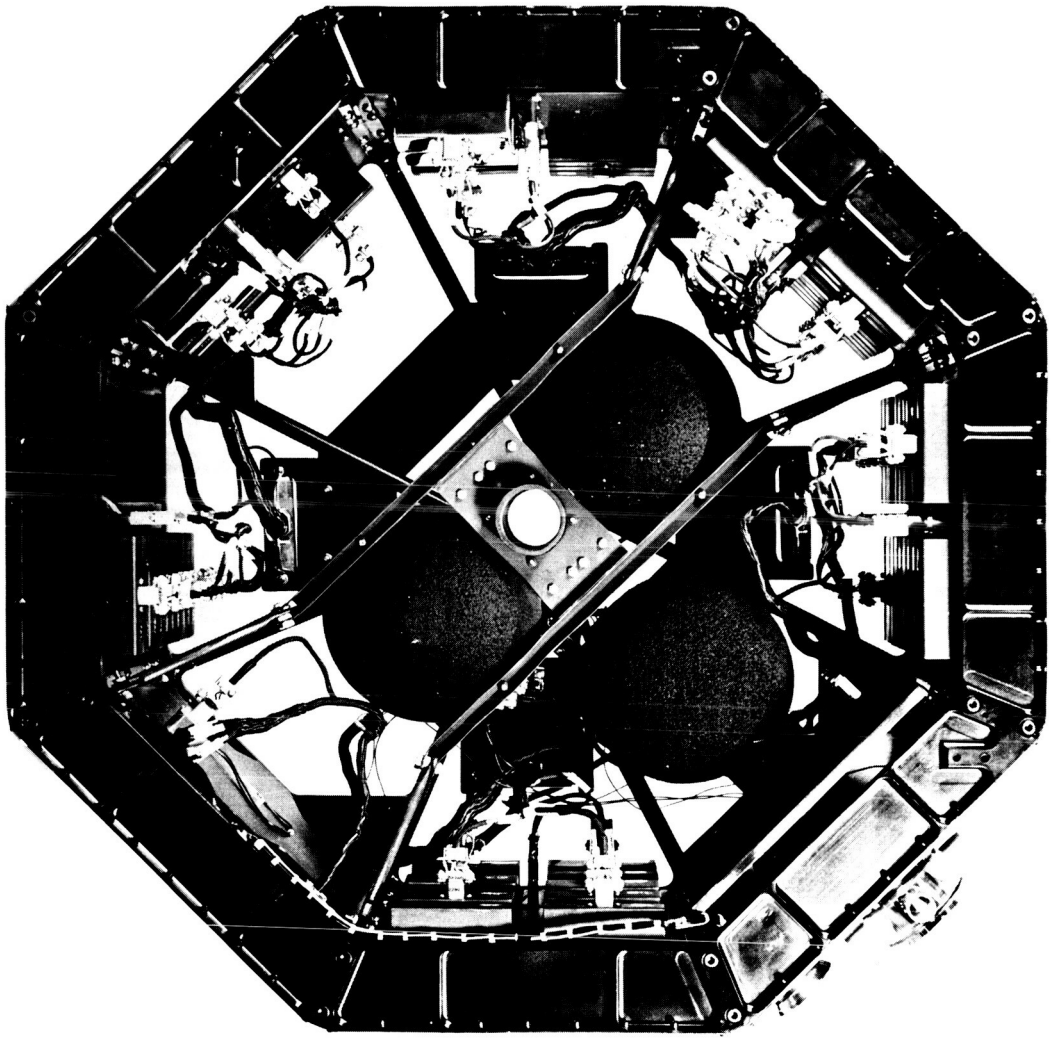

FIGURE 5 BOTTOM VIEW - TSM BUS

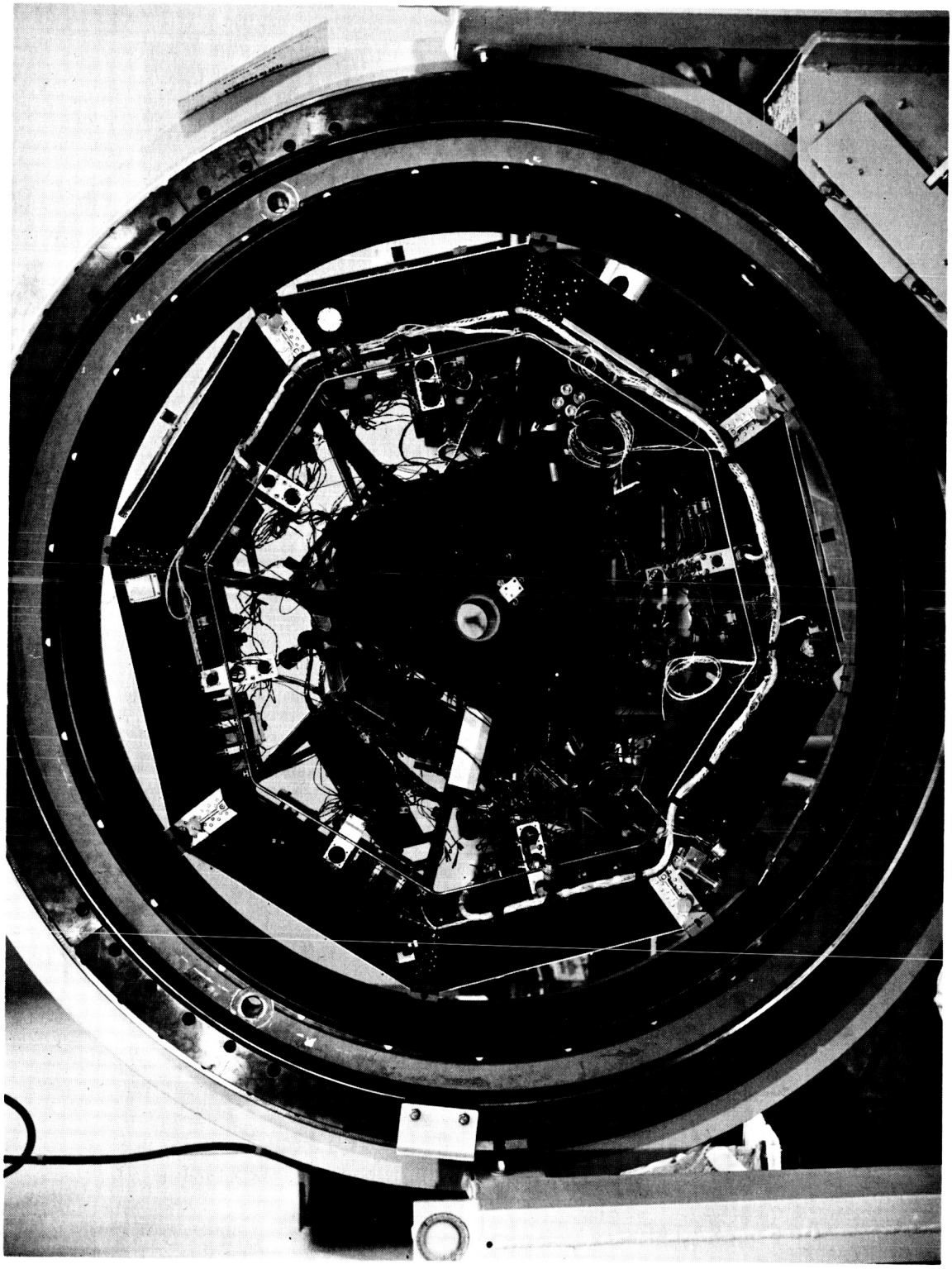

FIGURE 6 BOTTOM VIEW - TCM BUS

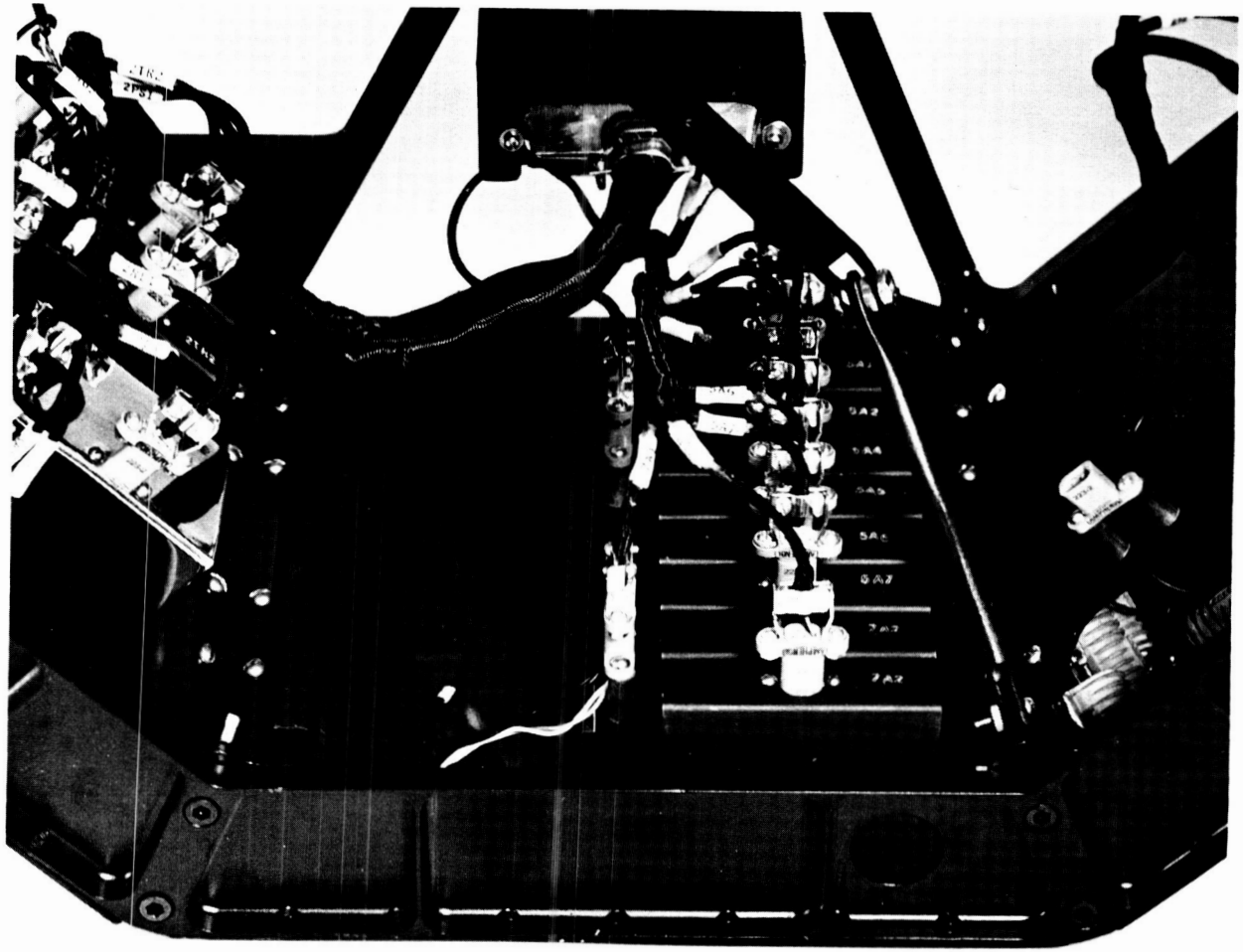

FIGURE 7 INTERIOR VIEW - TSM

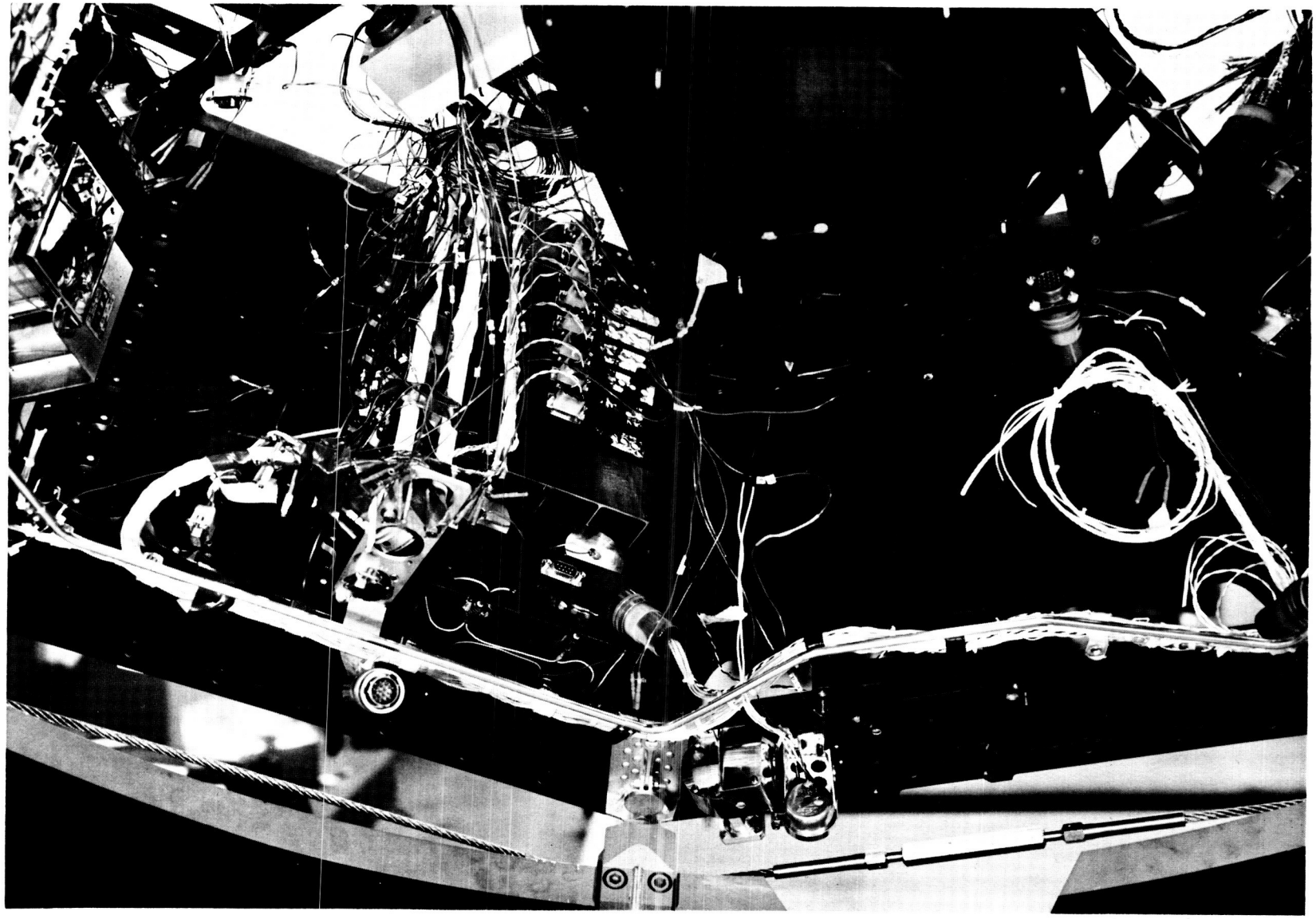

FIGURE 8 INTERIOR VIEW - TCM

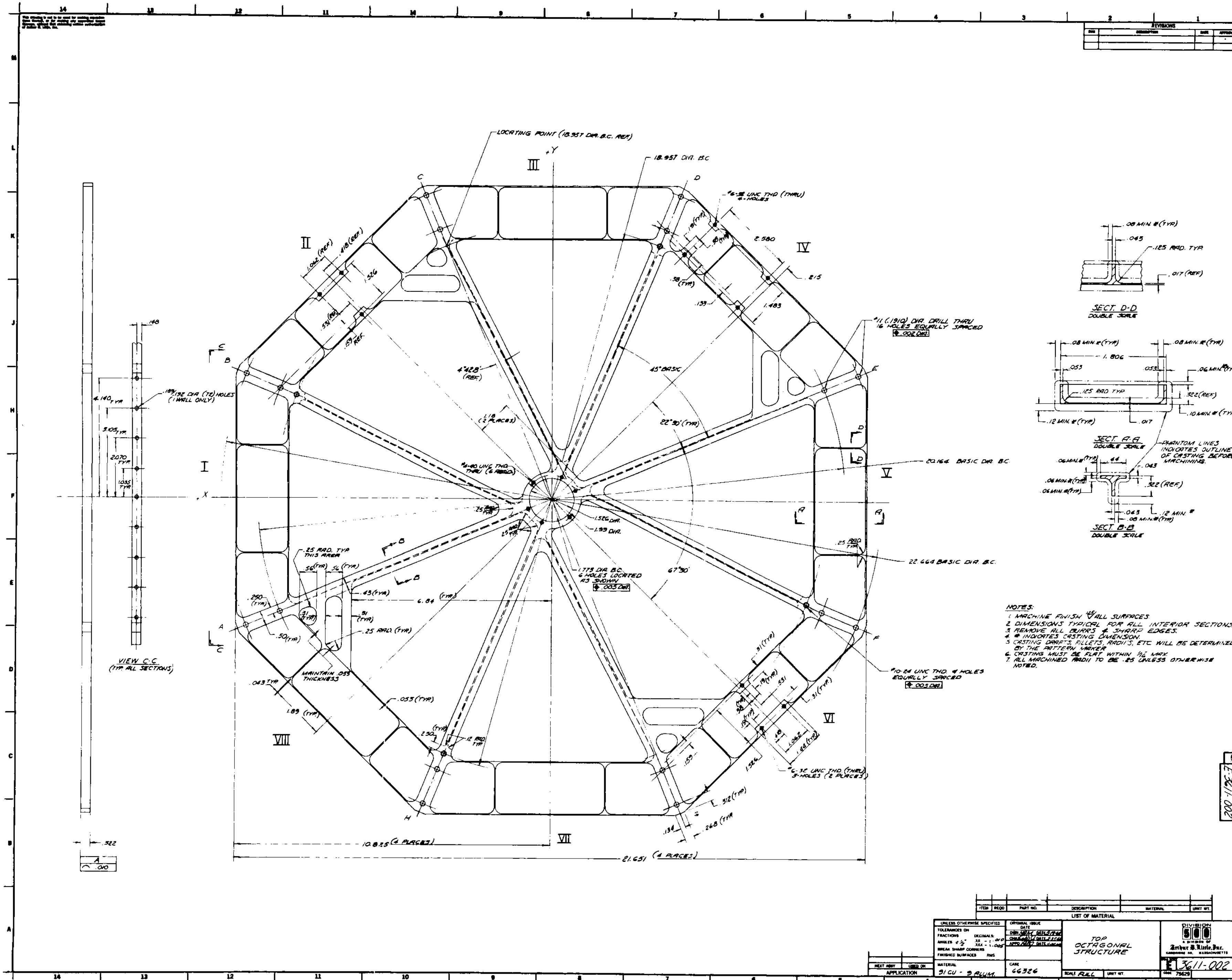

FIGURE 9 TOP OCTAGONAL FRAME

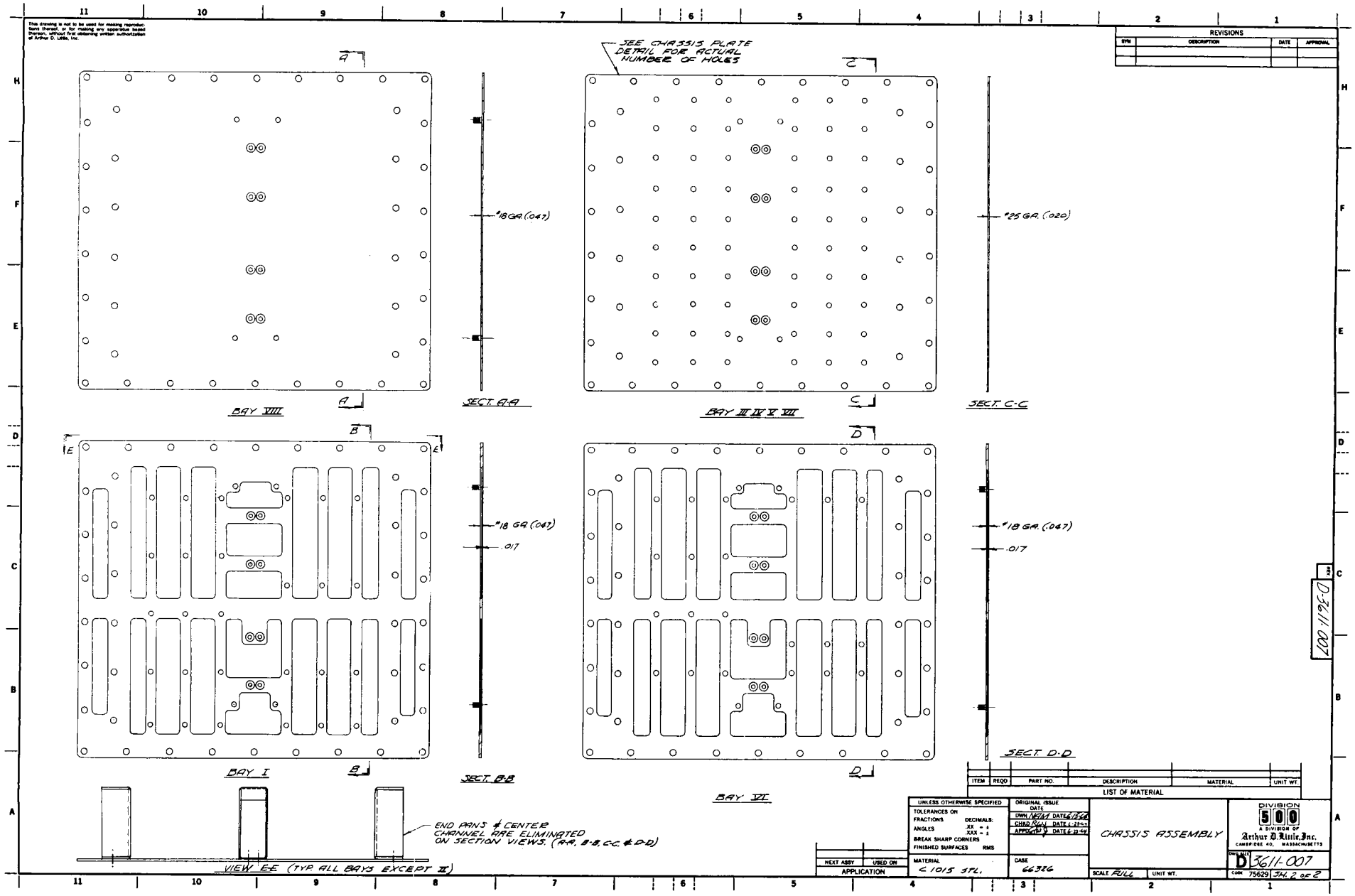

FIGURE 10 CHASSIS ASSEMBLY

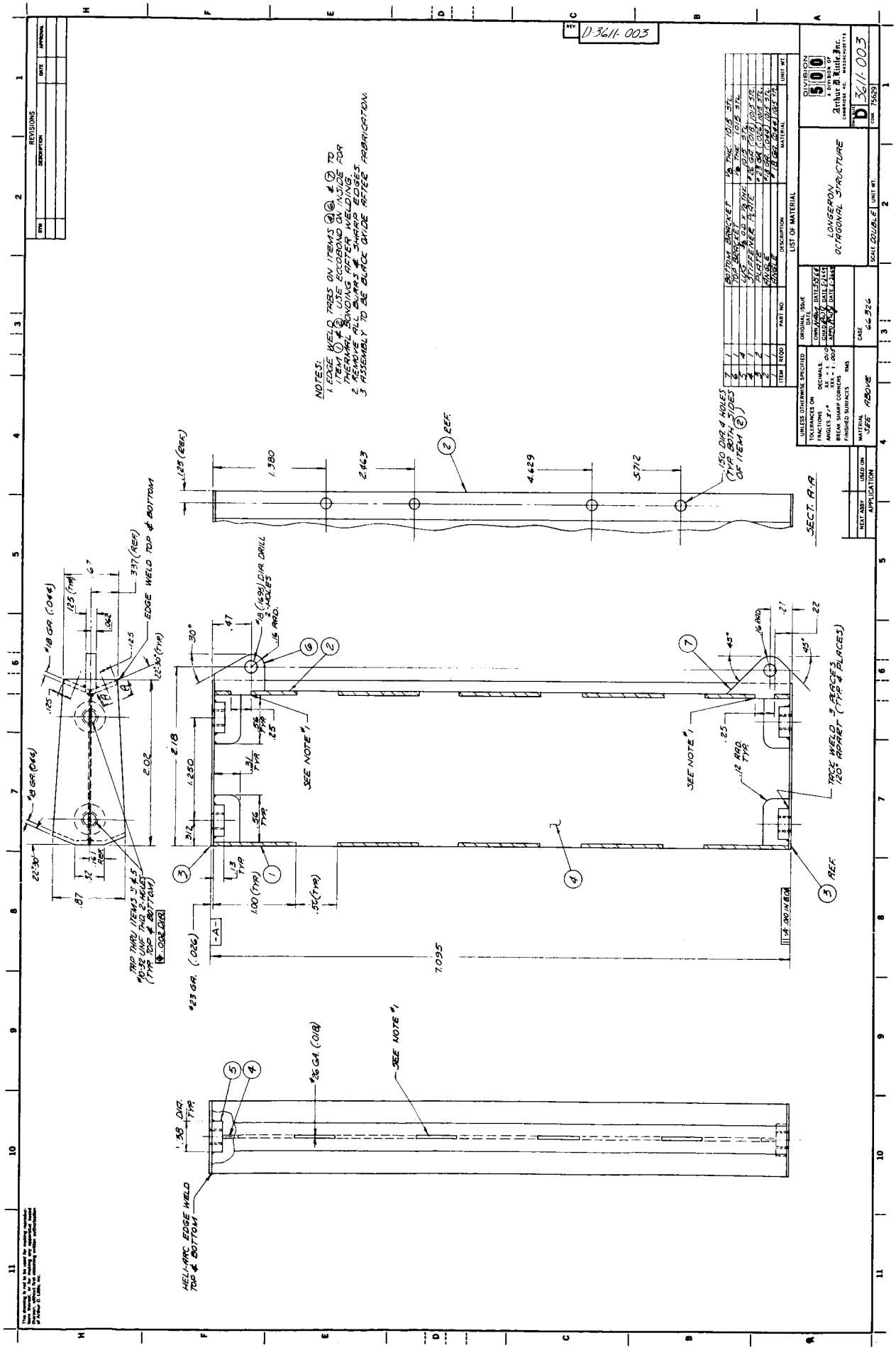

FIGURE 11 LONGERON

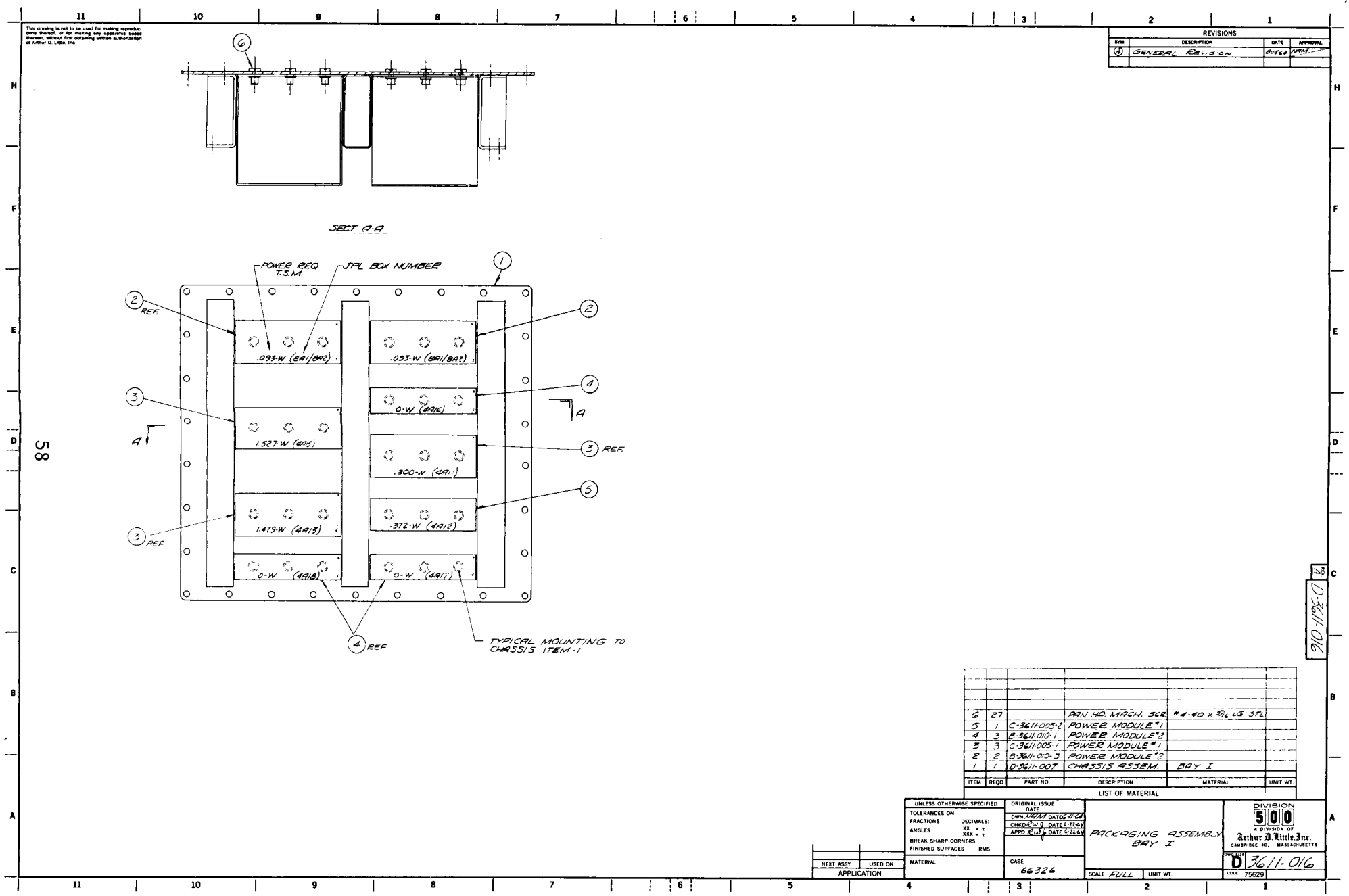

ITEM	REQD	PART NO.	DESCRIPTION	MATERIAL	UNIT WT.
6	27		PAN HD. MACH. SCR	#4-40 x 5/16 LG. STL.	
5	1	C-3611-005-2	POWER MODULE #1		
4	3	B-3611-010-1	POWER MODULE #2		
3	3	C-3611-005-1	POWER MODULE #1		
2	2	B-3611-010-3	POWER MODULE #2		
1	1	D-3611-007	CHASSIS ASSEM.	BAY I	

LIST OF MATERIAL

REVISIONS			
SYM	DESCRIPTION	DATE	APPROVAL
4	GENERAL REVISION	8-1-64	[illegible]

UNLESS OTHERWISE SPECIFIED
TOLERANCES ON FRACTIONS DECIMALS: .XX ± .1, .XXX ± .1
ANGLES ±
BREAK SHARP CORNERS
FINISHED SURFACES RMS
MATERIAL
ORIGINAL ISSUE DATE
DWN [illegible] DATE 6-17-64
CHKD R.W.S. DATE 6-22-64
APPD R.W.S. DATE 6-22-64
CASE 66326
NEXT ASSY | USED ON
APPLICATION

PACKAGING ASSEMBLY BAY I
SCALE FULL | UNIT WT.

DIVISION 500 A DIVISION OF Arthur D. Little, Inc. CAMBRIDGE 40, MASSACHUSETTS
DWG. SIZE D | 3611-016
CODE 75629

D-3611-016

58

FIGURE 12 PACKAGING ASSEMBLY BAY I

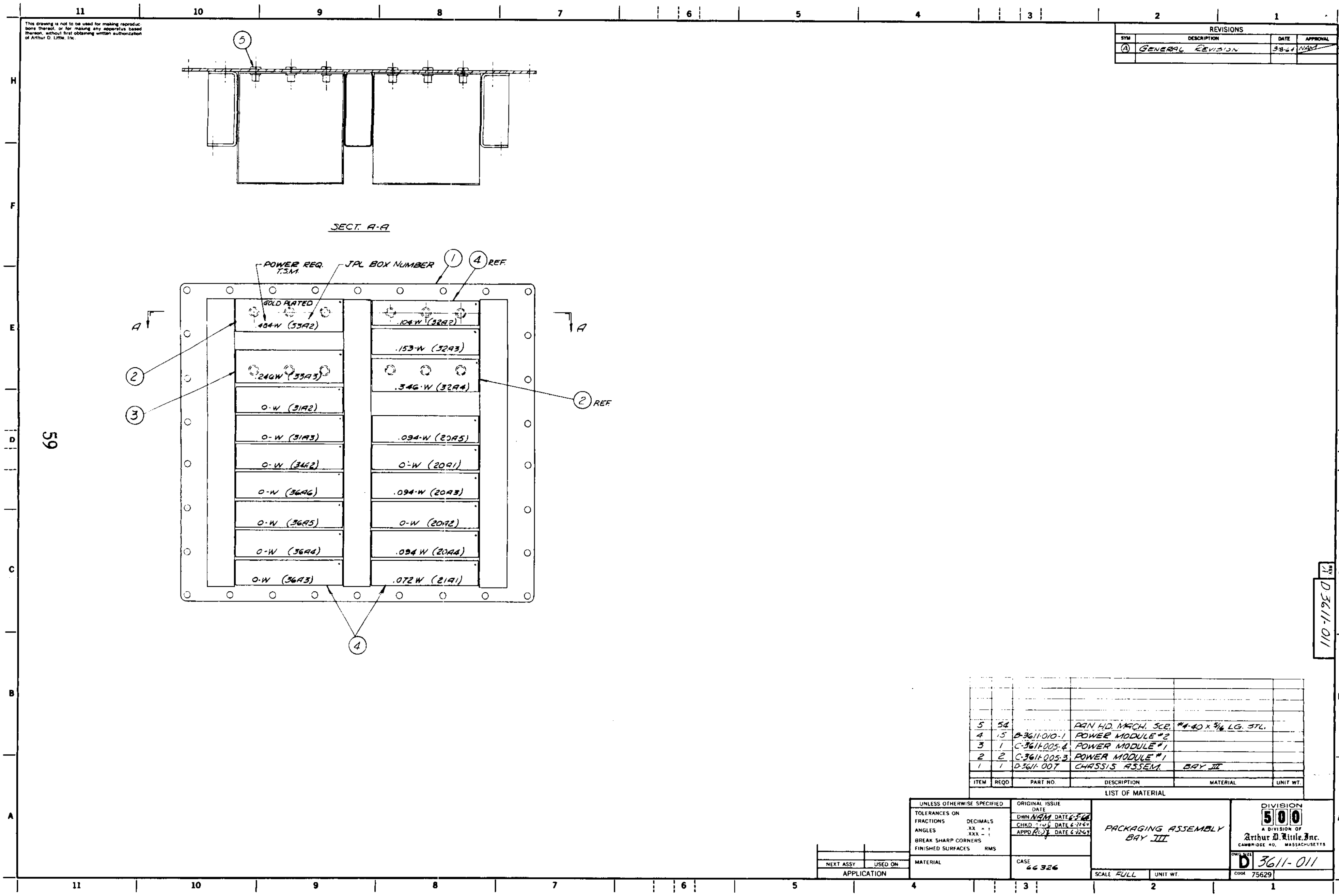

FIGURE 13 PACKAGING ASSEMBLY BAY III

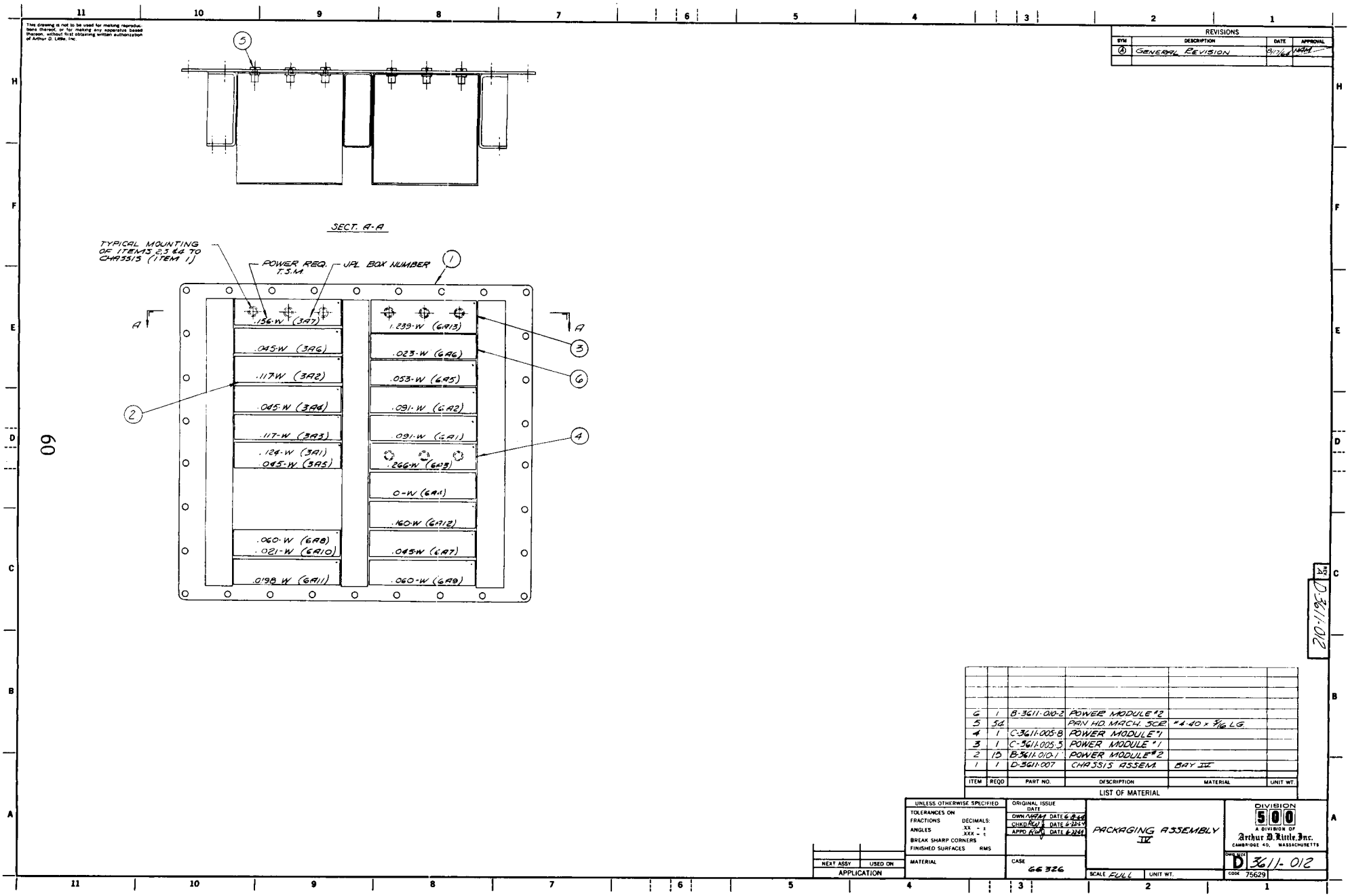

FIGURE 14 PACKAGING ASSEMBLY BAY IV

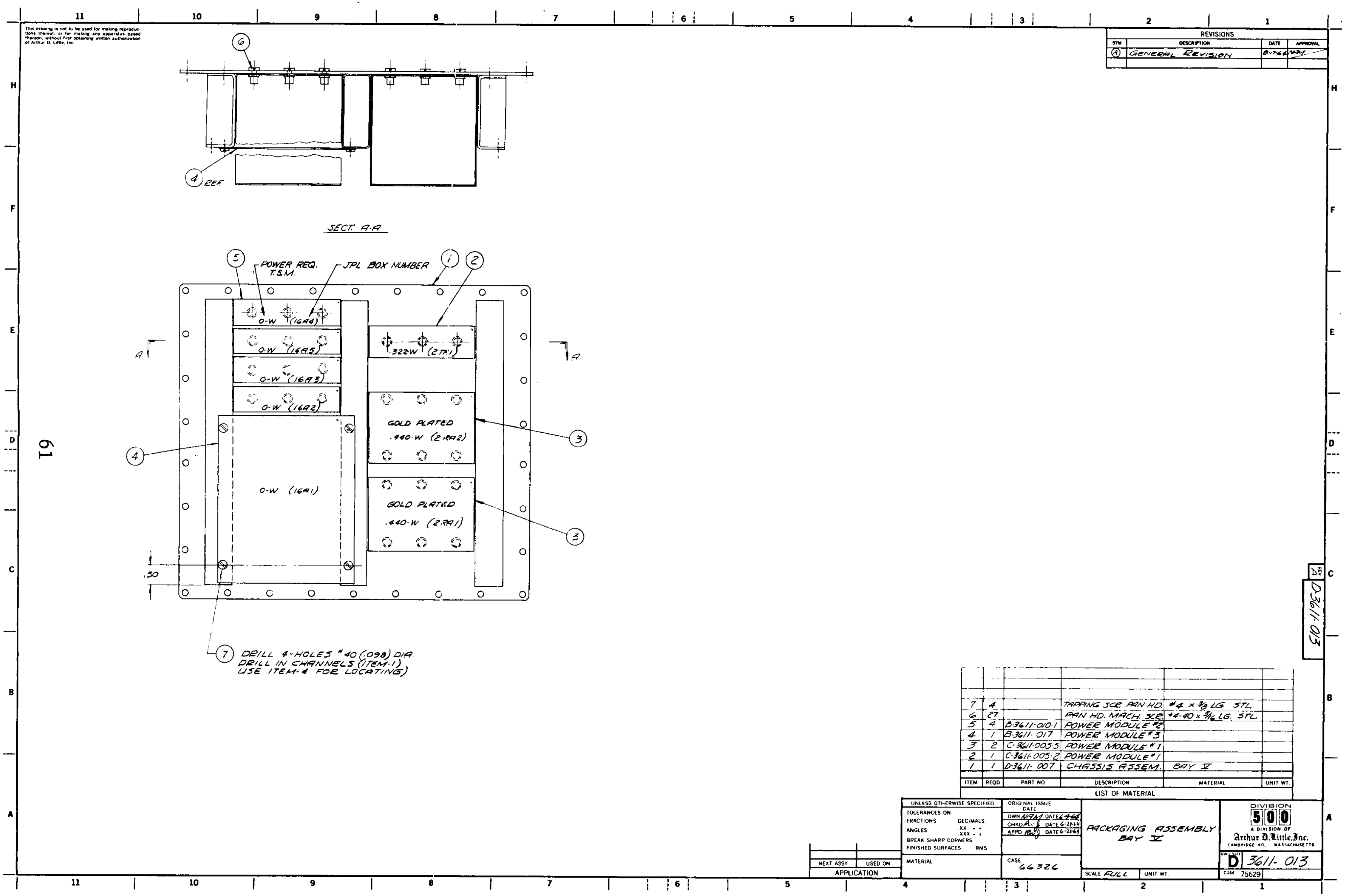

FIGURE 15 PACKAGING ASSEMBLY BAY V

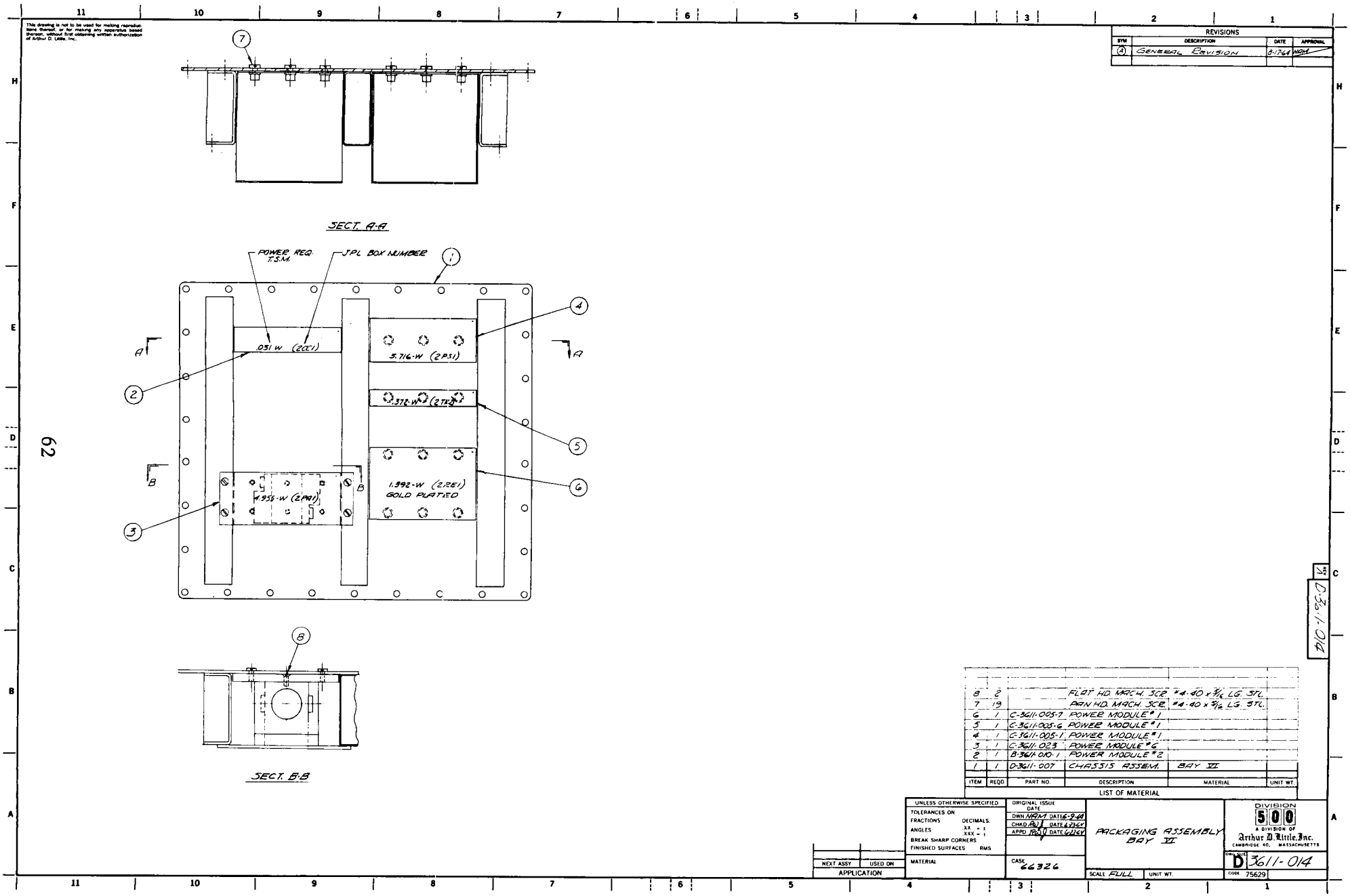

FIGURE 16 PACKAGING ASSEMBLY BAY VI

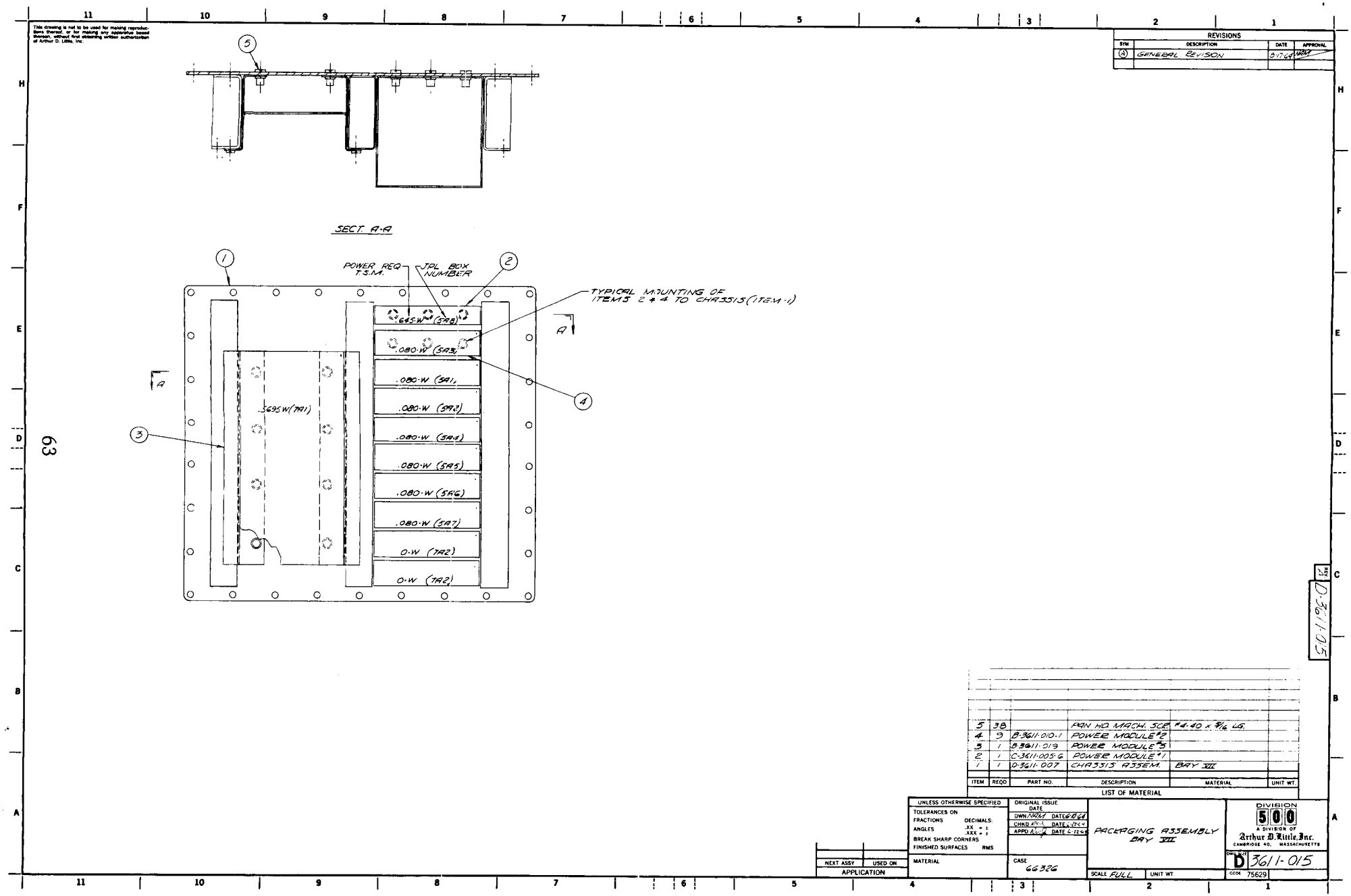

FIGURE 17 PACKAGING ASSEMBLY BAY VII

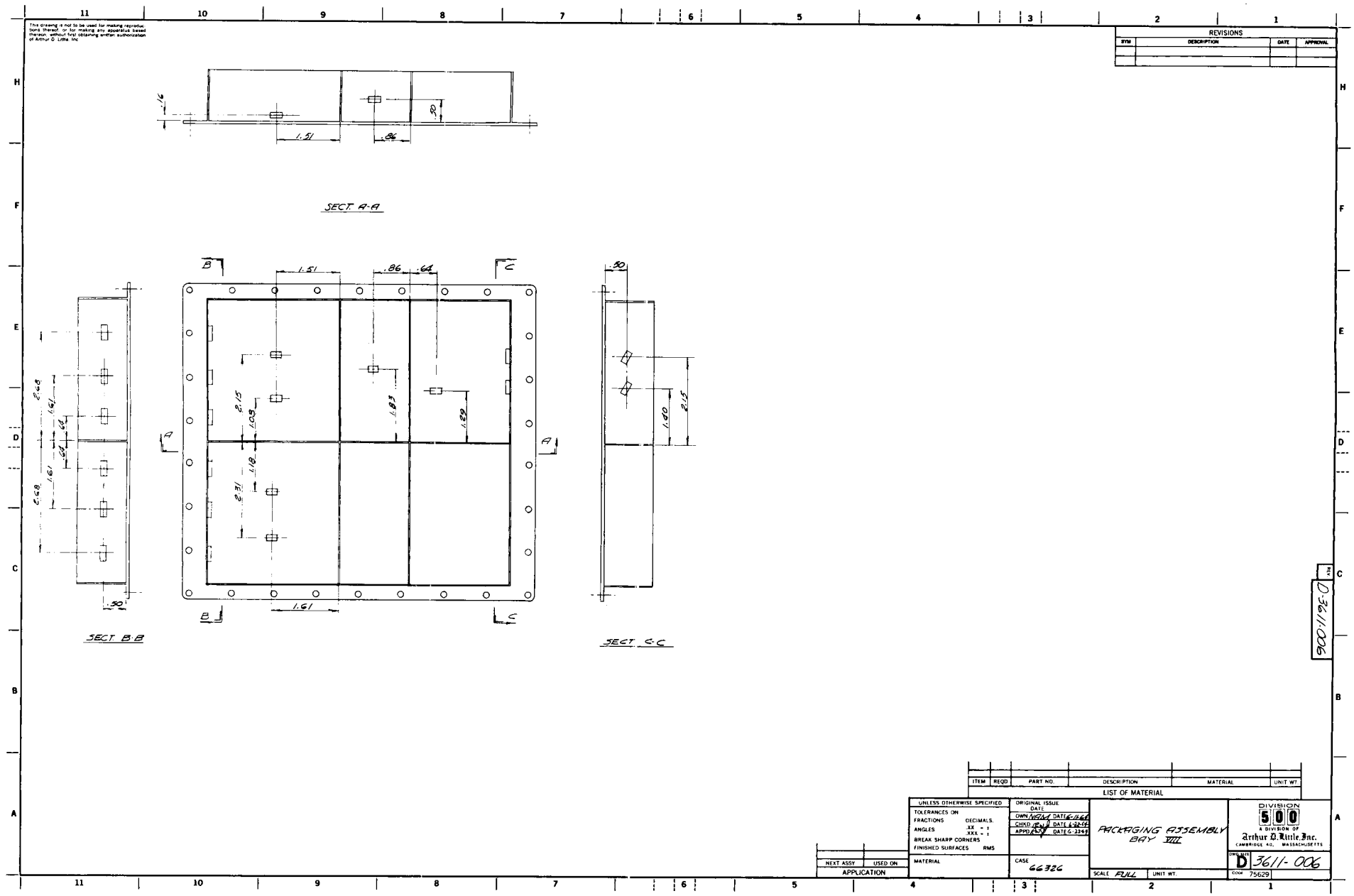

FIGURE 18 PACKAGING ASSEMBLY BAY VIII

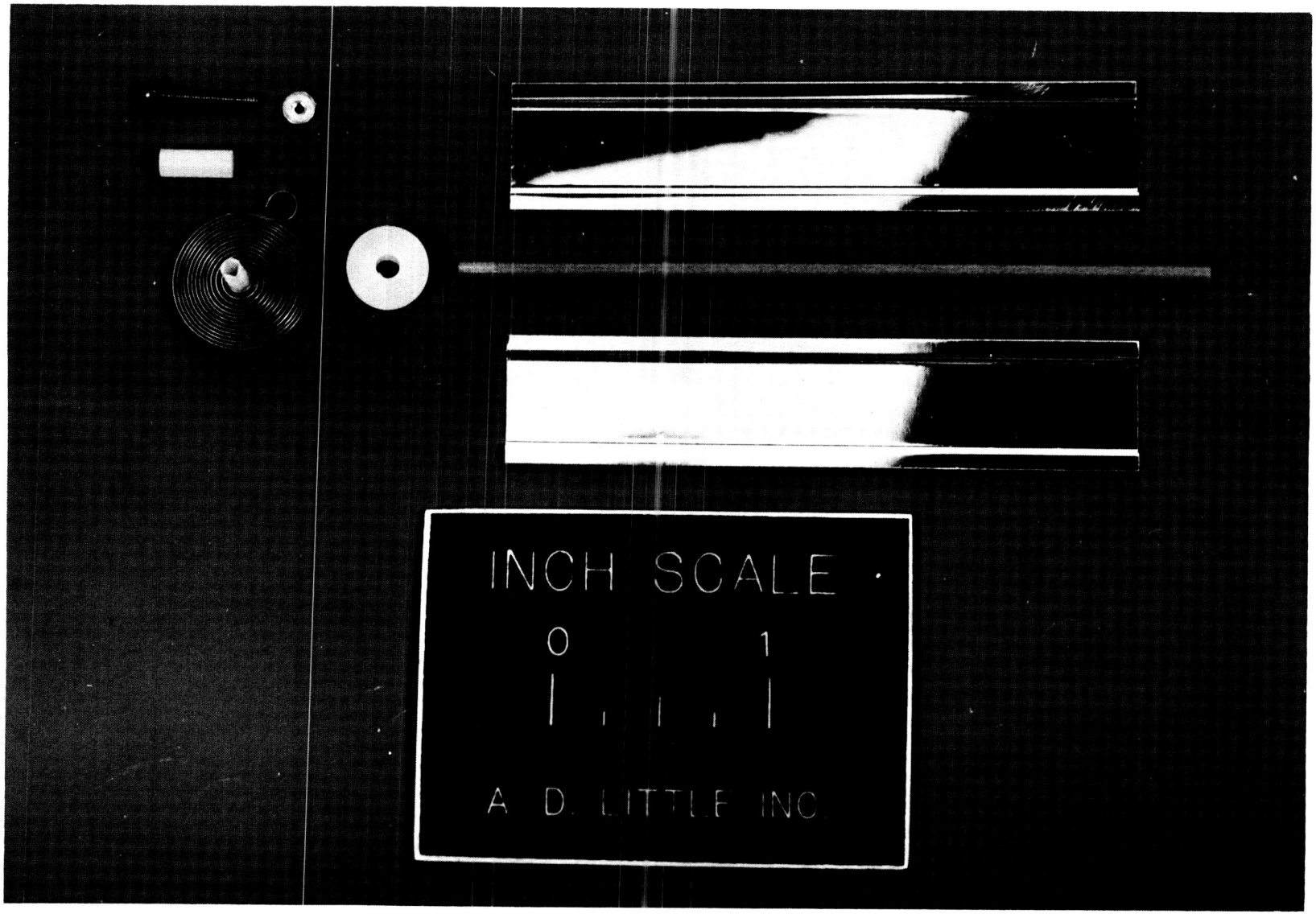

FIGURE 19 THERMAL CONTROL LOUVER BLADE ASSEMBLY

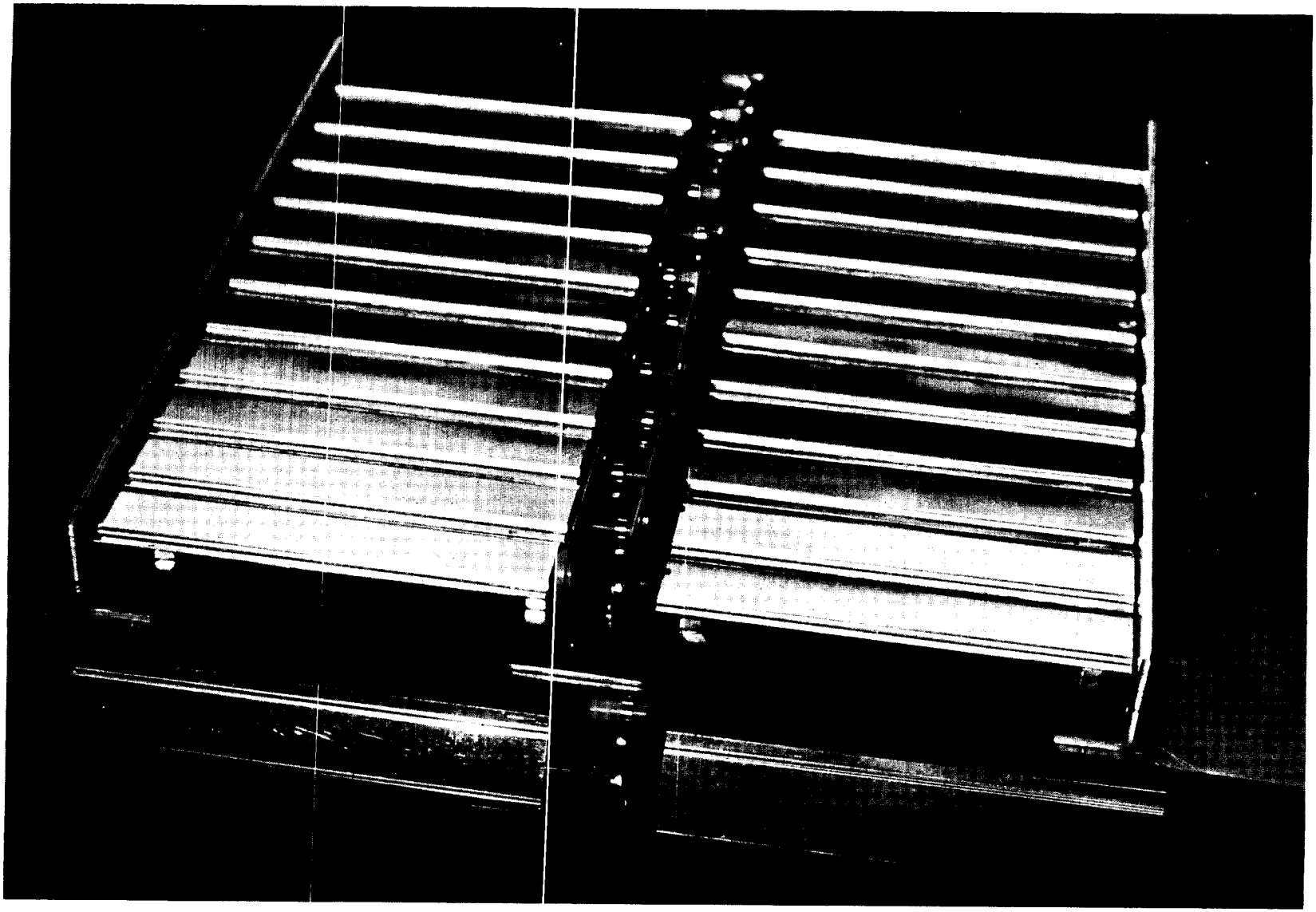

FIGURE 20 THERMAL CONTROL LOUVER ASSEMBLY

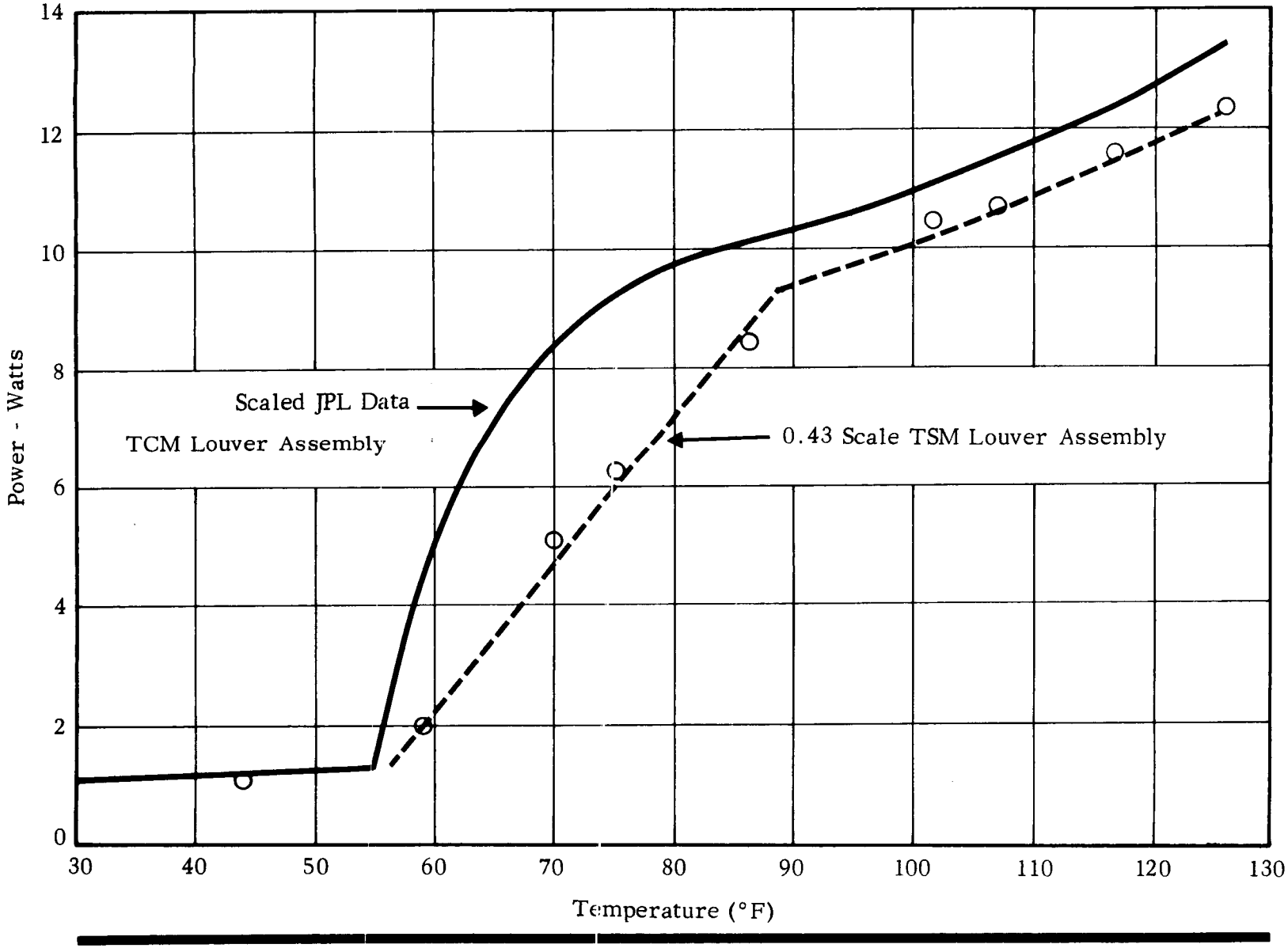

FIGURE 21 THERMAL CONTROL LOUVER PERFORMANCE

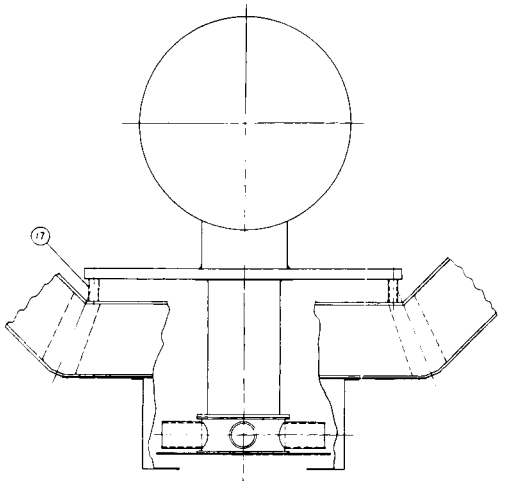

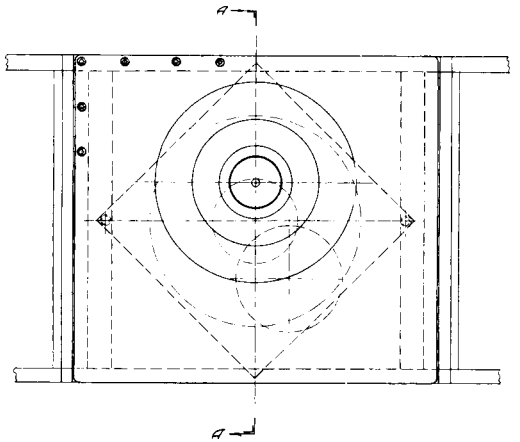

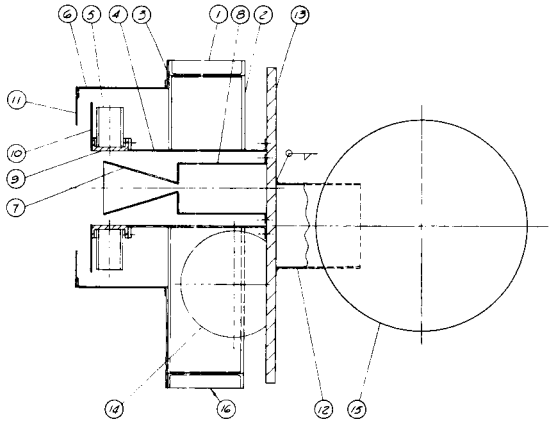

SECT A-A

NOTES:
1. ITEM 11 TO BE ATTACHED TO ITEM 6 WITH 3M ADHESIVE EC2216.
2. ITEM 10 TO BE ATTACHED TO ITEM 9 WITH ECCOBOND 56C ADHESIVE.
3. ITEM 7 TO BE SOFT SOLDERED TO ITEM 8.
4. I.D. OF ITEM 9 TO BE GOLD PLATED.
5. INSIDE SURFACE OF ITEM 7 TO BE POLISHED.
6. ITEM 14 ATTACHED TO ITEM 13 WITH 3M ADHESIVE EC2216.
7. ITEM 5 ATTACHED TO ITEM 9 WITH 3M ADHESIVE EC2216.
8. ITEMS 12, 15, 16 & 13 TO BE PAINTED WITH 3M SATIN BLACK.
9. OUTSIDE SURFACE OF ITEM 4 & 5 TO BE POLISHED.

ITEM	REQD	PART NO.	DESCRIPTION	MATERIAL	UNIT WT.
17	E		SPACER	1900 x .036 w EQUI-TE	
16	1	E-3611-004	LOWER OCTAGONAL STRUT	CASTING 31CU, 9AL	
15	1		BALL	.5 DIA. STYROFOAM	
14	1		BALL	.25 DIA. STYROFOAM	
13	1		HEATER	36 THRT ALUM EQUI-TE	
12	1		TUBING	2.00 x .035 w ALLAN 6061-TE	
11	1		DISC	.003 - .005 ALUM.	
10	1		DISC	.003 - .005 ALUM.	
9	1		RING	304 ST. STL.	
8	1		TUBING	1/4 OD x .042 w 321 ST. STL.	
7	1		NOZZLE	.006 THK 304 ST. STL.	
6	1		HOUSING	*26 GA. (.019) 410 ST. STL.	
5	4		TUBING	3/8 OD x .049 w EQUI-TE	
4	1		TUBING	1.750 DIA x .035 w 304 ST. STL.	
3	1		CHASSIS	*20 GA (.038) 410 ST. STL.	
2	8 (Ref)	E-3611-003	LONGERON	10.5 STL.	
1	1	E-3611-002	TOP OCTAGONAL STRUT	COMPOSITE 2.6# (Ref)	

LIST OF MATERIAL

UNLESS OTHERWISE SPECIFIED: TOLERANCES ON FRACTIONS ±1/64, DECIMALS .XX ±.1, .XXX ±.05, ANGLES ±1°, BREAK SHARP CORNERS, FINISHED SURFACES RMS

ORIGINAL ISSUE DATE
DRWN [illegible] DATE 6-6-69
CHKD [illegible] DATE 6-12-69
APPD [illegible] DATE 6-17-69

MATERIAL

CAGE

NEXT ASSY | USED ON APPLICATION

POST INJECTION PROPULSION SYSTEM (PIPS)

SCALE FULL | UNIT WT

DIVISION A DIVISION OF Arthur D. Little, Inc. CAMBRIDGE 40, MASSACHUSETTS

SIZE E | 3611-009 | REV

CODE 75670

E-3611-009

FIGURE 22 POST INJECTION PROPULSION SYSTEM

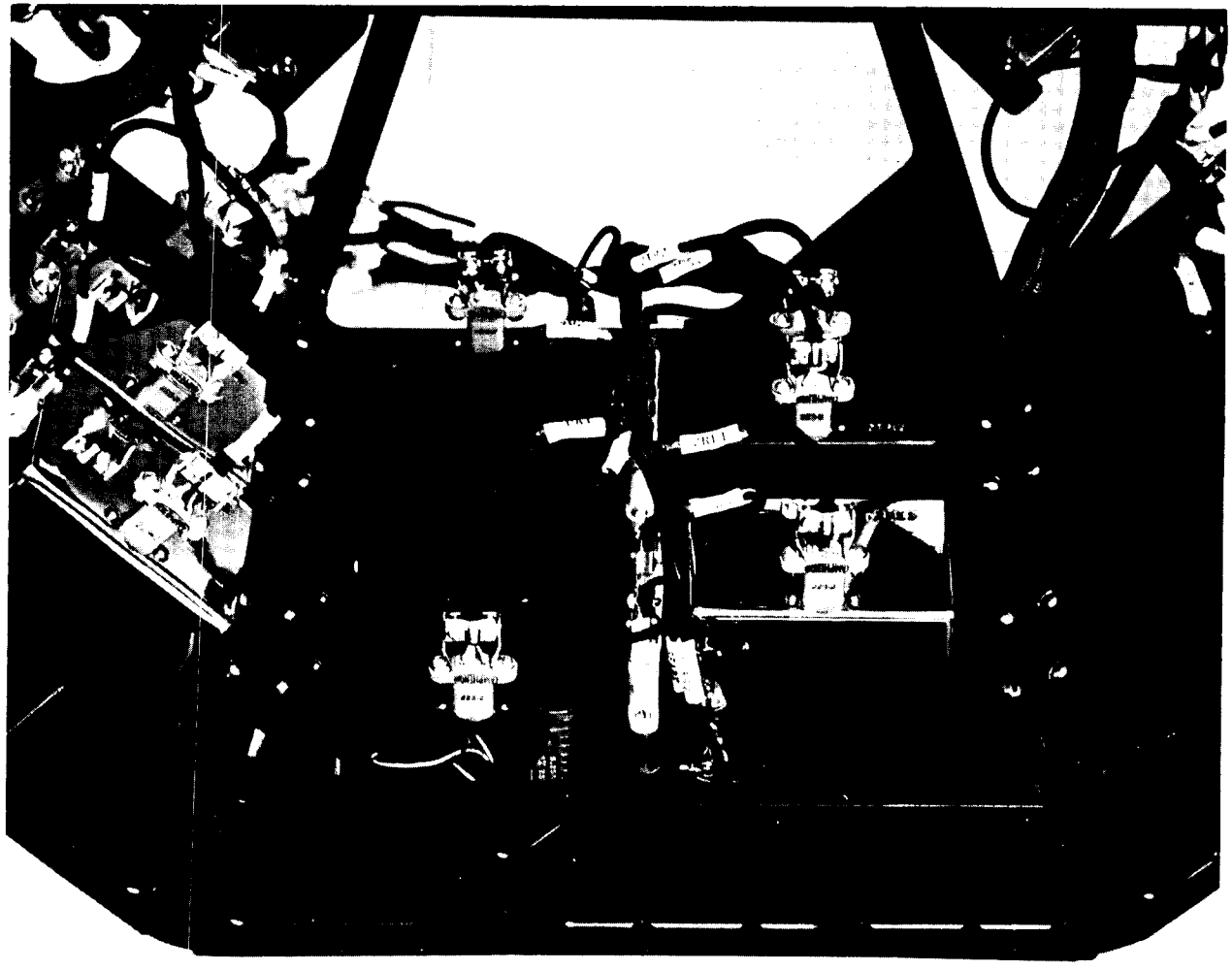

FIGURE 23 BAY 6 CONFIGURATION - TEST 3

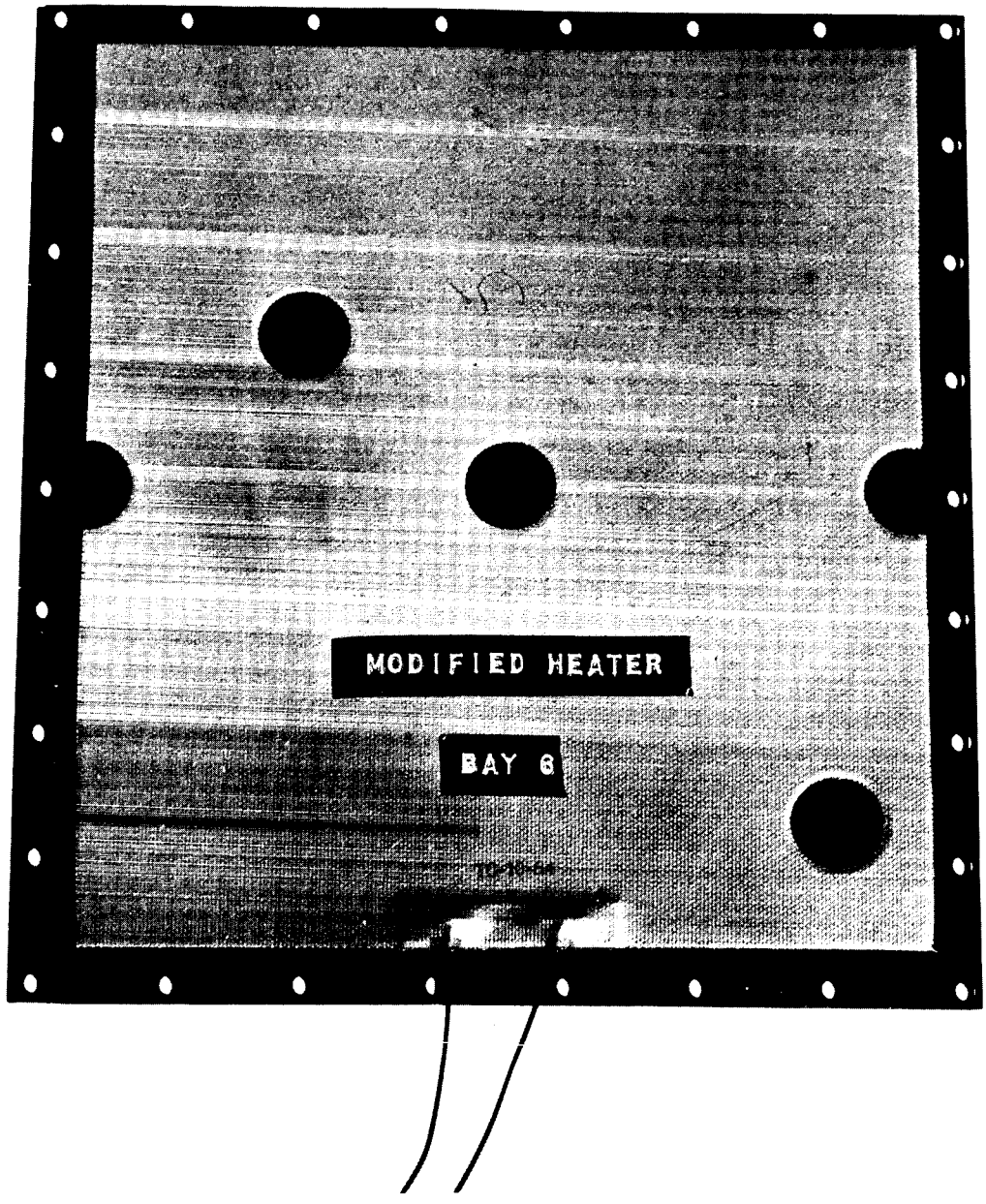

FIGURE 24 MODIFIED BAY 6 CONFIGURATION - TEST 4

APPENDIX I

TSM POWER BREAKDOWN

BAY I - POWER SUBSYSTEM

D 3611-016

Identification	TSM Power (Watts)	Number of Resistors
Pyrotechnic Control (8A1/8A2)	.093	1
Inverter (4A15)	1.527	2
Battery Charger (4A13)	1.479*	2
Inverter 4A18	0	0
Pyrotechnic Control 8A1/8A2	.093	1
Power Distribution (4A11)	.299	1
Power Synchronizer (4A12)	.372	1
Inverter (4A17)	0	0
Total Power (Earth Cruise)	3.864	
Total Power (Mars Cruise)	2.385	

* 4A13 dissipates 1.479 watts at Earth Cruise Mode and 0 watt at Mars Cruise.

BAY II - PIPS

This bay has no power dissipation.

BAY III - SCIENTIFIC EQUIPMENT

D 3611-011

Identification	TSM Power (Watts)	Number of Resistors
Magnetometer Electronics (33A2)	.484	2
Magnetometer Electronics (33A3)	.246	1
Scan Electronics (31A2)	0	0
Scan Electronics (31A3)	0	0
U. V. Electronics (34A2)	0	0
T. V. Power Supply (36A6)	0	0
Analog - Digital T.V. Encoder (36A5)	0	0
Deflection and Control (36A4)	0	0
Video Channels and Computer (36A3)	0	0
Plasma Electronics 1 (32A2)	.104	1
Plasma Electronics 2 (32A3)	.153	2
Plasma Electronics 3 (32A4)	.346	1
DAS Power Supply (20A5)	.094	1
Buffer Memory (20A1)	0	0
NRT DAS Logic (20A3)	.094	1
RT DAS Logic (20A2)	0	0
RT DAS Logic (20A4)	.094	1
Cosmic Ray Telescope (21A1)	.072	1
	1.686	

BAY IV - DATA ENCODER

D 3611-012

Identification	TSM Power (Watts)	Number of Resistors
Command Decoder and Power Supply (3A7)	.156	1
Command Decoder 2 (3A6)	.045	1
Command Detector 2 (3A2)	.117	1
Command Program Control (3A4)	.045	1
Command Detector 3 (3A3)	.117	1
Command Decoder 1 (3A5)	.045	1
Command Detector 1 (3A1)	.124	1
Decks 210, 220 (6A8)	.060	1
Decks 400, 410 (6A10)	.021	1
Decks 420, 430 (6A11)	0.0198	1
Power Supply (6A13)	1.239	3
Functional Switching (6A6)	.023	1
Event Counters (6A5)	.053	1
Modulator, Mixer, Transfer Register, Data Selector (6A2)	.091	1
PN Generators (6A1)	.091	1
Analog to Digital Converter (6A3)	.266	1
Analog to Digital Converter (6A4)	0	0
Low Level Amplifier (6A12)	.160	1
Decks 100, 110 (6A7)	.045	1
Decks 200, 300 (6A9)	.060	1
	2.7798	

BAY V - RECEIVER AND TAPE MACHINE

D 3611-013

Identification	TSM Power (Watts)	Number of Resistors
Tape Electronics 3 and TR (16A4)	0	0
Tape Electronics 4 (16A5)	0	0
Tape Electronics 2 (16A3)	0	0
Tape Electronics 1 (16A2)	0	0
Tape Machine (16A1)	0	0
Receiver Transformer Rectifier (2TRI)	.322	1
Receiver Subass'y. (2RA2)	.440	2
Receiver Subass'y. (2RA1)	.440	2
	1.202	

BAY VI - RF COMMUNICATIONS

D 3611-014

Identification	TSM Power (Watts)	Number of Resistors
Control Unit Subass'y. (2CC1)	.031	2
Power Amplifiers Subass'y. (2PA1)	4.955	2
Power Amplifiers Power Sup. (2PS1)	3.716	2
Exciters Transformer Rectifier (2TR2)	.372	1
Exciters (2RE1)	1.392	4
	10.466	

BAY VII - ATTITUDE CONTROL AND CC&S

D 3611-015

Identification	TSM Power (Watts)	Number of Resistors
Attitude Control Electronics (7A1)	0.5695	1
CC&S Transformer Rectifier (5A8)	.645	2
End Counter (5A3)	.080	1
Central Clock (5A1)	.080	1
Launch Counter (5A2)	.080	1
Maneuver Clock (5A4)	.080	1
Maneuver Duration (5A5)	.080	
Address Register and Maneuver Duration Output (5A6)	.080	1
Input Decoder (5A7)	.080	1
Gyro Control Ass'y. (7A2)	0	0
	1.7745	

BAY VIII - POWER REGULATOR ASSEMBLY

D 3611-006

Identification	TSM Power (Watts)	Number of Resistors
Maneuver Booster	0	0
Main Booster	3.328	3
Battery Diode	0	0
Solar Panel Diodes	.740	6
Electronics	1.405	7
	5.473	

TSM THERMOCOUPLE LIST

Phase II Configuration

JPL No.	Location
242	Bus tube at bottom
243	Bus tube at top
245	Bay 4 A/C nitrogen bottle, top
246	Bay 8 A/C nitrogen bottle, bottom
248	Bay 1, 4A15
249	Bay 1, chassis at 4A15
250	Bay 1, 4A13
303	Bay 1, 4A17
305	Bay 2, midcourse nozzle near throat
306	Bay 2, midcourse inside jet vane ring
307	Bay 2, propellant tank
309	Bay 2, umbilical connector
310	Bay 2, shear plate
311	Bay 3, 33A2
316	Bay 3, 32A4
322	Bay 3, chassis centerline top
323	Bay 3, chassis centerline center
324	Bay 3, chassis centerline bottom
329	Bay 4, 6A13
330	Bay 4, chassis at 6A13
332	Bay 4, 6A9
333	Bay 4, flight
336	Bay 5, 2TR1
337	Bay 5, 2RA1
340	Bay 5, chassis centerline top
341	Bay 5, chassis centerline center
342	Bay 5, chassis centerline bottom
345	Bay 6, 2PA1 case

JPL No.	Location
347	Bay 6, chassis at 2PA1
348	Bay 6, 2PS1
349	Bay 6, chassis at 2PS1
350	Bay 6, 2RE1
401	Bay 6, chassis centerline top
402	Bay 6, chassis centerline center
403	Bay 6, chassis centerline bottom
406	Bay 7, 7A1, one-third down
412	Bay 7, 7A2, gyro #2
415	Bay 7, 5A8
418	Bay 7, flight
419	Bay 8, solar panel diodes (upper, bay 7 side)
420	Bay 8, solar panel diodes (lower, bay 7 side)
422	Bay 8, main booster (upper, bay 1 side)
423	Bay 8, vertical centerline top
425	Bay 8, vertical centerline bottom
426	Bay 8, battery case
451*	Hat Center
452*	Hat Edge Bay 6
453*	Hat Edge Bay 2
454*	Flight Shield Bay 5

* ADL Numbering System--not used by JPL.